Low SNR Asymptotic Rates of Vector Channels With One-Bit Outputs

Amine Mezghani, *Member, IEEE*, Josef A. Nossek, *Life Fellow, IEEE*, and A. Lee Swindlehurst, *Fellow, IEEE*

***Abstract*— We analyze the performance of multiple-input multiple-output (MIMO) links with one-bit output quantization in terms of achievable rates and characterize their performance loss compared to unquantized systems for general channel statistical models and general channel state information (CSI) at the receiver. One-bit ADCs are particularly suitable for large-scale millimeter wave MIMO Communications (massive MIMO) to reduce the hardware complexity. In such applications, the signal-to-noise ratio per antenna is rather low due to the propagation loss. Thus, it is crucial to analyze the performance of MIMO systems in this regime by means of information-theoretical methods. Since an exact and general information-theoretic analysis is not possible, we resort to the derivation of a general asymptotic expression for the mutual information in terms of a second-order expansion around zero SNR. We show that up to second order in the SNR, the mutual information of a system with two-level (sign) output signals incorporates only a power penalty factor of $\pi/2$ (1.96 dB) compared to systems with infinite resolution for all channels of practical interest with perfect or statistical CSI. An essential aspect of the derivation is that we do not rely on the common pseudo-quantization noise model.**

***Index Terms*— Massive MIMO communication, broadband regime, one-bit quantization, mutual information, optimal input distribution, ergodic capacity, millimeter-wave communications.**

I. Introduction

IN THIS paper, we investigate the theoretically achievable rates under one-bit analog-to-digital conversion (ADC) at the receiver for a wide class of channel models. To this end, we consider general multi-antenna communication channels with coarsely quantized outputs and general communication scenarios, e.g. correlated fading, full and statistical channel state information (CSI) at the transmitter and the receiver, etc.. Since exact capacity formulas are intractable in such quantized channels, we resort to a low signal-to-noise ratio (SNR) approximation and lower bounds on the channel capacity to perform the analysis. Such mutual information asymptotics can be utilized to evaluate the performance of quantized output channels or design and optimize the system in practice. Additionally, the low SNR analysis under coarse quantization is useful in the context of large scale (or massive) multiple-input multiple-output (MIMO) [4], [5] and millimeter-wave (mmwave) communications [6]–[10], considered as key enablers to achieve higher data rates in future wireless networks. In fact, due to high antenna gains possible with massive MIMO and the significant path-loss at mmwave frequencies, such systems will likely operate at rather low SNR values at each antenna, while preferably utilizing low-cost hardware and low-resolution ADCs, in order to access all available dimensions even at low precision. Our asymptotic analysis demonstrates that the capacity degradation due to quantized sampling is surprisingly small in the low SNR regime for most cases of practical interest.

Manuscript received December 7, 2017; revised May 23, 2020; accepted September 9, 2020. Date of publication October 13, 2020; date of current version November 20, 2020. This work was supported in part by the German Research Foundation (DFG) under the priority Program SPP1202 and in part by the U.S. National Science Foundation under Grant CCF-1703635 and Grant ECCS-1824565. *(Corresponding author: Amine Mezghani.)*

Amine Mezghani is with the Department of Electrical and Computer Engineering, University of Manitoba, Winnipeg, MB R3T 2N2, Canada (e-mail: amine.mezghani@umanitoba.ca).

Josef A. Nossek is with the Department of Electrical and Computer Engineering, Technical University of Munich, 80333 Munich, Germany, and also with the Federal University of Ceará, Fortaleza 60020-181, Brazil (e-mail: josef.a.nossek@tum.de).

A. Lee Swindlehurst was with the Institute for Advanced Study, Technical University of Munich, 85748 Garching bei München, Germany. He is now with the Department of EECS, University of California at Irvine, Irvine, CA 92697 USA (e-mail: swindle@uci.edu).

Communicated by M. K. Varanasi, Associate Editor for Communications.

Color versions of one or more of the figures in this article are available online at https://ieeexplore.ieee.org.

Digital Object Identifier 10.1109/TIT.2020.3030855

A. Less Precision for More Dimensions: The Motivation for Coarse Quantization

The use of low resolution (e.g., one-bit) ADCs and DACs is a potential approach to significantly reducing cost and power consumption in massive MIMO wireless transceivers. It was proposed as early as 2006 by [11]- [14] in the context of conventional MIMO. In the last three years however, the topic has gained significantly increased interest by the research community [15]- [47] as an attractive low cost solution for large vector channels. In the extreme case, a one-bit ADC consists of a simple comparator and consumes negligible power. One-bit ADCs do not require an automatic gain control and the complexity and power consumption of the gain stages required prior to them are substantially reduced [48]. Ultimately, one-bit conversion is, in view of current CMOS technology, the only conceivable option for a direct mmwave bandpass sampling implementation close to the antenna, eliminating the need for power-intensive radio-frequency (RF) components such as mixers and oscillators. In addition, the use of one-bit ADCs not only simplifies the interface to the antennas by relaxing the RF requirements but also simplifies the interface between the converters and the digital processing unit (DSP/FPGA).

0018-9448 © 2020 IEEE. Personal use is permitted, but republication/redistribution requires IEEE permission.
See https://www.ieee.org/publications/rights/index.html for more information.

Authorized licensed use limited to: Access paid by The UC Irvine Libraries. Downloaded on May 08,2021 at 22:45:13 UTC from IEEE Xplore. Restrictions apply.

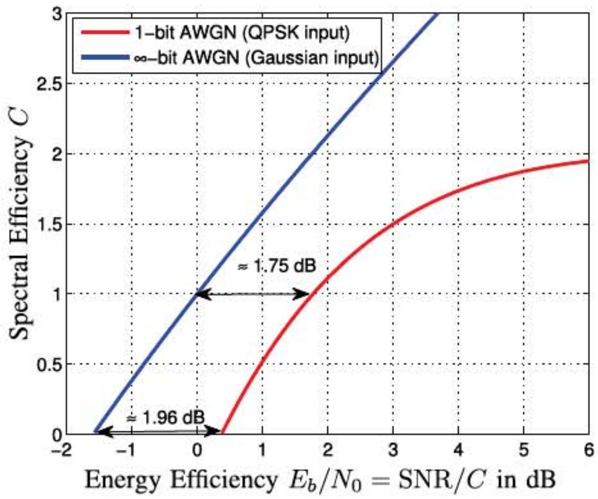

Fig. 1. Spectral efficiency versus energy efficiency for One- and Infinite-Bit Quantization in AWGN channels.

For instance, the use of 10-bit converters running at 1 Gsps for 100 antennas would require a data pipeline of 1 Tbit/s to the FPGAs and a very complex and power-consuming interconnect. By using only one-bit quantization the speed and complexity are reduced by a factor of 10. Sampling with one-bit ADCs might therefore qualify as a fundamental research area in communication theory.

Even though the use of only a single quantization bit, *i.e.*, simply the sign of the sampled signal, is a severe nonlinearity, initial research has shown that the theoretical "best-case" performance loss that results with a one-bit quantizer is not as significant as might be expected, at least at low SNRs where mmwave massive MIMO is expected to operate, prior to the beamforming gain, which can still be fully exploited. This is also very encouraging in the context of low-cost and low-power IoT devices which will also likely operate in relatively low SNR regimes. Fig. 1 shows how the theoretical spectral efficiency versus energy efficiency (E_b/N_0) of a one-bit transceiver that uses QPSK symbols in an additive white Gaussian noise (AWGN) channel compares with that of an infinite-precision ADC using a Gaussian input, i.e. the Shannon limit $\log_2(1+\mathrm{SNR})$. In fact, the capacity of the one-bit output AWGN channel is achieved by QPSK signals and reads as [20], [49]

$$C_{1-\mathrm{bit}} = 2\left(1 - H_b(\Phi(\sqrt{\mathrm{SNR}}))\right), \quad (1)$$

where we make use of the binary entropy function $H_b(p) = -p \cdot \log_2\ p - (1-p)\cdot\log_2(1-p)$ and the cumulative Gaussian distribution $\Phi(z)$. Surprisingly, at low SNR the loss due to one-bit quantization is approximately equal to only $\pi/2$ (1.96dB) [49], [50] and actually decreases to roughly 1.75dB at spectral efficiency of about 1 bit per complex dimension, which corresponds to the spectral efficiency of today's 3G systems.

Even if a system is physically equipped with higher resolution converters and high-performance RF-chains, situations may arise where the processing of desired signals must be performed at a much lower resolution, due for instance to the presence of a strong interferer or a jammer with a greater dynamic range than the signals of interest. In fact, after subtracting or zero-forcing the strong interferer, the residual effective number of bits available for the processing of other signals of interest is reduced substantially. Since future wireless systems must operate reliably even under severe conditions in safety-critical applications such as autonomous driving, investigating communication theory and signal processing under coarse quantization of the observations is crucial.

B. Related Work and Contributions

Many contributions have studied MIMO channels operating in Rayleigh fading environments in the unquantized (infinite resolution) case, for both the low SNR [50]–[55] and high SNR [56] regimes. Such asymptotic analyses are very useful since characterizing the achievable rate for the whole SNR regime is in general intractable. This issue becomes even more difficult in the context of one-bit quantization at the receiver side, apart from very special cases. In the works [1], [14], the effects of quantization were studied from an information-theoretic point of view for MIMO systems, where the channel is perfectly known at the receiver. These works demonstrated that the loss in channel capacity due to coarse quantization is surprisingly small at low to moderate SNR. In [2], [3], the block fading single-input single-output (SISO) non-coherent channel was studied in detail. The work of [25] provided a general capacity lower bound for quantized MIMO and general bit resolutions that can be applied for several channel models with perfect CSI, particularly with correlated noise. The achievable capacity for the AWGN channel with output quantization has been extensively investigated in [19], [20], and the optimal input distribution was shown to be discrete. The authors of [18] studied the one-bit case in the context of an AWGN channel and showed that the capacity loss can be fully recovered when using asymmetric quantizers. This is however only possible at extremely low SNR, which might not be useful in practice. In [57], it was shown that, as expected, oversampling can also reduce the quantization loss in the context of band-limited AWGN channels. In [21], non-regular quantizer designs for maximizing the information rate are studied for intersymbol-interference channels. More recently, [28] studied bounds on the achievable rates of MIMO channels with one-bit ADCs and perfect channel state information at the transmitter and the receiver, particularly for the multiple-input single-output (MISO) channel. The recent work of [47] analyzes the sum capacity of the two-user multiple access SISO AWGN channel, which turns out to be achievable with time-division and power control.

Motivated by these works, we aim to study and characterize the communication performance of point-to-point MIMO channels with general assumptions about the channel state information at the receiver taking into account the 1-bit quantization as a deterministic operation. In particular, we derive asymptotics for the mutual information up to the second-order in the SNR and study the impact of quantization. We show that up to second order in SNR for all channels of practical interest, the mutual information of a system with two-level (1-bit sign operation) output signals incorporates only a power penalty of

Authorized licensed use limited to: Access paid by The UC Irvine Libraries. Downloaded on May 08,2021 at 22:45:13 UTC from IEEE Xplore. Restrictions apply.

$\frac{\pi}{2}$ (−1.96 dB) compared to a system with infinite resolution. Alternatively, to achieve the same rate with the same power up to the second-order as in the ideal case, the number of one-bit output dimensions has to be increased by a factor of $\pi/2$ for the case of perfect CSI and at least by $\pi^2/4$ for the statistical CSI case, while essentially no increase in the number of transmit dimensions is required. We also characterize analytically the compensation of the quantization effects by increasing the number of 1-bit receive dimensions to approach the ideal case.

This paper is organized as follows: Section II describes the system model. Then, Section III provides the main theorem consisting of a second-order asymptotic approximation of the entropy of one-bit quantized vector signals. In Section IV, we provide a general expression for the mutual information between the inputs and the quantized outputs of the MIMO system with perfect channel state information, then we expand that into a Taylor series up to the second-order in the SNR. In Section V, we extend these results to elaborate on the asymptotic capacity of 1-bit MIMO systems with statistical channel state information including Rayleigh flat-fading environments with delay spread and receive antenna correlation.

C. Notation

Vectors and matrices are denoted by lower and upper case italic bold letters. The operators $(\bullet)^{\mathrm{T}}$, $(\bullet)^{\mathrm{H}}$, $\mathrm{tr}(\bullet)$, $(\bullet)^*$, $\mathrm{Re}(\bullet)$ and $\mathrm{Im}(\bullet)$ stand for transpose, Hermitian (conjugate transpose), matrix trace, complex conjugate, real and imaginary parts of a complex number, respectively. The terms $\mathbf{0}_M$ and $\mathbf{1}_M$ denote the M-dimensional vectors of all zeros and all ones, respectively, while $\boldsymbol{I}_M$ represents the identity matrix of size M. The vector $\boldsymbol{x}_i$ is the i-th column of matrix $\boldsymbol{X}$ and $x_{i,j}$ denotes its (ith, jth) element, while x_i is the i-th element of the vector $\boldsymbol{x}$ and $\boldsymbol{x}_{n:m} = [x_n, \cdots, x_m]^{\mathrm{T}}$. The quantity $\|\boldsymbol{x}\|_0$ denotes the number of non-zero elements in the vector $\boldsymbol{x}$. The operator $\mathrm{E}[\bullet]$ stands for expectation with respect to all random variables, while the operator $\mathrm{E}_{s|q}[\bullet]$ stands for the expectation with respect to the random variable s given q. In addition, $\boldsymbol{C}_x = \mathrm{E}[\boldsymbol{x}\boldsymbol{x}^{\mathrm{H}}] - \mathrm{E}[\boldsymbol{x}]\mathrm{E}[\boldsymbol{x}^{\mathrm{H}}]$ represents the covariance matrix of $\boldsymbol{x}$ and $\boldsymbol{C}_{xy}$ denotes $\mathrm{E}[\boldsymbol{x}\boldsymbol{y}^{\mathrm{H}}]$. The functions $P(s)$ and $P(s|q)$ symbolize the joint probability mass function (pmf) and the conditional pmf of s and q, respectively. Additionally, $\mathrm{diag}(\boldsymbol{A})$ denotes a diagonal matrix containing only the diagonal elements of $\boldsymbol{A}$ and $\mathrm{nondiag}(\boldsymbol{A}) = \boldsymbol{A} - \mathrm{diag}(\boldsymbol{A})$. Finally, we represent element-wise multiplication and the Kronecker product of vectors and matrices by the operators "$\circ$" and "$\otimes$", respectively. Throughout the paper, low SNR expansions of entropy and mutual information are given in nats.

II. System Model

We consider a point-to-point quantized MIMO channel with M transmit dimensions (e.g. antennas or, more generally, spatial and temporal dimensions) and N dimensions at the receiver. Fig. 2 shows the general form of a quantized MIMO system, where $\boldsymbol{H} \in \mathbb{C}^{N\times M}$ is the channel matrix, whose distribution is known at the receiver side. The channel realizations are in general unknown to both the transmitter and receiver, except for the ideal perfect-CSI case. The vector $\boldsymbol{x} \in \mathbb{C}^M$ comprises the M transmitted symbols, assumed to be subject to an average power constraint $\mathrm{E}[\|\boldsymbol{x}^2\|] \leq P_{\mathrm{Tr}}$. The vector $\boldsymbol{\eta}$ represents the additive noise, whose entries are i.i.d. and distributed as $\mathcal{CN}(0, \sigma_\eta^2)$. The quantized channel output $\boldsymbol{r} \in \mathbb{C}^N$ is thus represented as

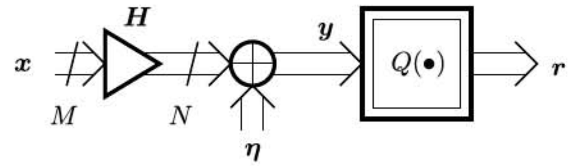

Fig. 2. Quantized MIMO System.

$$\boldsymbol{r} = Q(\boldsymbol{y}) = Q(\boldsymbol{H}\boldsymbol{x} + \boldsymbol{\eta}). \tag{2}$$

In a one-bit system, the real parts $y_{i,R}$ and the imaginary parts $y_{i,I}$ of the unquantized receive signals y_i, $1 \leq i \leq N$, are each quantized by a symmetric one-bit quantizer. Thus, the resulting quantized signals read as

$$r_{i,c} = Q(y_{i,c}) = \mathrm{sign}(y_{i,c}) = \begin{cases} +1 & \text{if } y_{i,c} \geq 0 \\ -1 & \text{if } y_{i,c} < 0, \end{cases} \tag{3}$$

for $c \in \{R, I\}$, $1 \leq i \leq N$. The operator $Q(\boldsymbol{y})$ will also be denoted as $\mathrm{sign}(\boldsymbol{y})$ and represents the one-bit symmetric scalar quantization process in each real dimension. The restriction to one-bit symmetric quantization is motivated by its simple implementation. Since all of the real and imaginary components of the receiver noise $\boldsymbol{\eta}$ are statistically independent with variance σ_η^2, we can express each of the conditional probabilities as the product of the conditional probabilities on each receiver dimension

$$\begin{aligned} P(\boldsymbol{r} = \mathrm{sign}(\boldsymbol{y})|\boldsymbol{x}, \boldsymbol{H}) &= \prod_{c\in\{R,I\}} \prod_{i=1}^{N} P(r_{i,c}|\boldsymbol{x}, \boldsymbol{H}) \\ &= \prod_{c\in\{R,I\}} \prod_{i=1}^{N} \Phi\left(\frac{r_{i,c}[\boldsymbol{H}\boldsymbol{x}]_{i,c}}{\sqrt{\sigma_\eta^2/2}}\right), \end{aligned} \tag{4}$$

where $\Phi(x) = \frac{1}{\sqrt{2\pi}} \int_{-\infty}^{x} e^{-\frac{t^2}{2}} dt$ is the cumulative normal distribution function. We first state the main theorem used throughout the paper and then provide the asymptotics of the mutual information for several channel models up to second order in the SNR.

III. Main Theorem for the Asymptotic Entropy of One-Bit Quantized Vector Signals

We provide a theorem that can be used for deriving the second order approximation of the mutual information. It considers the 1-bit signal $\boldsymbol{r} = \mathrm{sign}(\varepsilon\boldsymbol{x} + \boldsymbol{\eta})$, where $\boldsymbol{x}$ is a random vector with a certain distribution and $\boldsymbol{\eta}$ is random with i.i.d. Gaussian entries and unit variance, while ε is a signal scaling parameter.

Theorem 1: Assuming $\boldsymbol{x} \in \mathbb{C}^N$ is a proper complex random vector ($\mathrm{E}[\boldsymbol{x}\boldsymbol{x}^{\mathrm{T}}] = \mathrm{E}[\boldsymbol{x}]\mathrm{E}[\boldsymbol{x}^{\mathrm{T}}]$) satisfying $\mathrm{E}_{\boldsymbol{x}}[\|\boldsymbol{x}\|_4^{4+\varepsilon}] < \delta$ for some finite constants $\varepsilon, \delta > 0$ and $\boldsymbol{\eta}$ is i.i.d. Gaussian with

Authorized licensed use limited to: Access paid by The UC Irvine Libraries. Downloaded on May 08,2021 at 22:45:13 UTC from IEEE Xplore. Restrictions apply.

unit variance, then the following entropy approximation holds up to the second order in ε^2

$$H(\text{sign}(\varepsilon \boldsymbol{x}+\boldsymbol{\eta})) = 2N\ln 2 - \frac{2}{\pi}\varepsilon^2 \|\mathrm{E}[\boldsymbol{x}]\|_2^2 - \varepsilon^4\left(\frac{2}{\pi^2}\mathrm{tr}\left((\text{nondiag}(\boldsymbol{C}_{\boldsymbol{x}}))^2\right) - \frac{4}{3\pi}\|\mathrm{E}[\boldsymbol{x}]\circ\mathrm{E}[\boldsymbol{x}\circ\boldsymbol{x}\circ\boldsymbol{x}]\|_1^1 + \frac{4}{3\pi^2}\|\mathrm{E}[\boldsymbol{x}]\|_4^4\right) + o(\varepsilon^4), \tag{5}$$

where $\|\boldsymbol{a}\|_p^p = \sum_{i,c}|a_{i,c}|^p$ and $[\boldsymbol{a}\circ\boldsymbol{b}]_i = a_{i,R}b_{i,R} + \mathrm{j}a_{i,I}b_{i,I}$, while the expectation is taken with respect to $\boldsymbol{x}$ and $\boldsymbol{C}_{\boldsymbol{x}} = \mathrm{E}[\boldsymbol{x}\boldsymbol{x}^{\mathrm{H}}] - \mathrm{E}[\boldsymbol{x}]\mathrm{E}[\boldsymbol{x}^{\mathrm{H}}]$ is the covariance matrix of $\boldsymbol{x}$.

Proof: See Appendix A. □

From this theorem, we can deduce some useful corollaries.

Corollary 1: For any possibly non-deterministic function $\boldsymbol{g}(\boldsymbol{x})$ satisfying $\mathrm{E}_{\boldsymbol{x}}[\|\boldsymbol{g}(\boldsymbol{x})\|_4^{4+\varepsilon}] < \delta$ and $\mathrm{E}[\boldsymbol{g}(\boldsymbol{x})\boldsymbol{g}(\boldsymbol{x})^{\mathrm{T}}] = \mathrm{E}[\boldsymbol{g}(\boldsymbol{x})]\mathrm{E}[\boldsymbol{g}(\boldsymbol{x}^{\mathrm{T}})]$ for some finite constants $\varepsilon, \delta > 0$, we have the following entropy expansion to the second order in ε^2

$$\begin{aligned} H(\text{sign}(\varepsilon \boldsymbol{g}(\boldsymbol{x})+\boldsymbol{\eta})) &= 2N\ln 2 - \frac{2}{\pi}\varepsilon^2\|\mathrm{E}[\boldsymbol{g}(\boldsymbol{x})]\|_2^2 \\ &\quad - \varepsilon^4\left(\frac{2}{\pi^2}\mathrm{tr}\left((\text{nondiag}(\boldsymbol{C}_{\boldsymbol{g}(\boldsymbol{x})}))\right)^2\right) \\ &\quad - \frac{4}{3\pi}\|\mathrm{E}[\boldsymbol{g}(\boldsymbol{x})]\circ\mathrm{E}[\boldsymbol{g}(\boldsymbol{x})\circ\boldsymbol{g}(\boldsymbol{x})\circ\boldsymbol{g}(\boldsymbol{x})]\|_1^1 \\ &\quad + \frac{4}{3\pi^2}\|\mathrm{E}[\boldsymbol{g}(\boldsymbol{x})]\|_4^4\Big) + \Delta H(\text{sign}(\varepsilon\boldsymbol{g}(\boldsymbol{x})+\boldsymbol{\eta})), \end{aligned}$$

where the remainder term $\Delta H(\text{sign}(\varepsilon\boldsymbol{g}(\boldsymbol{x})+\boldsymbol{\eta}))$ is $o(\varepsilon^4)$.

Corollary 2: For any function $\boldsymbol{g}(\boldsymbol{x})$ satisfying $\mathrm{E}_{\boldsymbol{x}}[\|\boldsymbol{g}(\boldsymbol{x})\|_4^{4+\varepsilon}] < \delta$ and $\mathrm{E}[\boldsymbol{g}(\boldsymbol{x})\boldsymbol{g}(\boldsymbol{x})^{\mathrm{T}}|\boldsymbol{x}] = \mathrm{E}[\boldsymbol{x}|\boldsymbol{x}]\,\mathrm{E}[\boldsymbol{g}(\boldsymbol{x})(\boldsymbol{x})^{\mathrm{T}}|\boldsymbol{x}]$, we have the following second order approximation of the conditional entropy

$$\begin{aligned} H(\text{sign}(\varepsilon \boldsymbol{g}(\boldsymbol{x})+\boldsymbol{\eta})|\boldsymbol{x}) &= 2N\ln 2 - \frac{2}{\pi}\varepsilon^2\mathrm{E}_{\boldsymbol{x}}[\|\mathrm{E}[\boldsymbol{g}(\boldsymbol{x})|\boldsymbol{x}]\|_2^2] \\ &\quad - \varepsilon^4\mathrm{E}_{\boldsymbol{x}}\Big[\frac{2}{\pi^2}\mathrm{tr}\left((\text{nondiag}(\boldsymbol{C}_{\boldsymbol{g}(\boldsymbol{x})|\boldsymbol{x}}))^2\right) \\ &\quad - \frac{4}{3\pi}\|\mathrm{E}[\boldsymbol{g}(\boldsymbol{x})|\boldsymbol{x}]\circ\mathrm{E}[\boldsymbol{g}(\boldsymbol{x})\circ\boldsymbol{g}(\boldsymbol{x})\circ\boldsymbol{g}(\boldsymbol{x})|\boldsymbol{x}]\|_1^1 \\ &\quad + \frac{4}{3\pi^2}\|\mathrm{E}[\boldsymbol{g}(\boldsymbol{x})|\boldsymbol{x}]\|_4^4\Big] + \Delta H(\text{sign}(\varepsilon\boldsymbol{g}(\boldsymbol{x})+\boldsymbol{\eta})|\boldsymbol{x}), \end{aligned}$$

where the remainder term $\Delta H(\text{sign}(\varepsilon\boldsymbol{g}(\boldsymbol{x})+\boldsymbol{\eta})|\boldsymbol{x})$ is $o(\varepsilon^4)$.

Proof: Corollary 1 is a direct result of Theorem 1, where we just replace the random vector $\boldsymbol{x}$ by $\boldsymbol{g}(\boldsymbol{x})$ if the stated conditions are fulfilled for $\boldsymbol{g}(\boldsymbol{x})$. For Corollary 2 we just perform the expectation in Theorem 1 first conditioned on $\boldsymbol{x}$, to get the entropy for a given $\boldsymbol{x}$ and then we take the average with respect to $\boldsymbol{x}$, again if the stated assumptions regarding the distribution of $\boldsymbol{g}(\boldsymbol{x})$ are fulfilled. These results will be used to derive a second order approximation of the mutual information of quantized MIMO systems for the case of perfect as well as statistical channel state information. The condition $\mathrm{E}_{\boldsymbol{x}}[\|\boldsymbol{g}(\boldsymbol{x})\|_4^{4+\alpha}] < \gamma$ for some finite constants α, $\gamma > 0$ ensures that the remainder term of the expansion satisfies

$$|\Delta H(\text{sign}(\varepsilon\boldsymbol{g}(\boldsymbol{x})+\boldsymbol{\eta})|\boldsymbol{x})| = \mathrm{E}_{\boldsymbol{x}}[o(\|\boldsymbol{g}(\boldsymbol{x})\|_4^4\varepsilon^4)] \le \gamma^{\frac{4+\alpha'}{4+\alpha}}\varepsilon^{4+\alpha'}, \tag{6}$$

for some $\alpha' \in]0,\alpha]$ and is therefore $o(\frac{1}{\sigma_\eta^4})$, which follows the explanation given in (109), Appendix A. □

IV. Mutual Information and Capacity With Full CSI

When the channel $\boldsymbol{H}$ is perfectly known at the receiver, the mutual information (in nats/s/Hz) between the channel input and the quantized output in Fig. 2 reads as [58]

$$I(\boldsymbol{x};\boldsymbol{r}|\boldsymbol{H}) = \mathrm{E}_{\boldsymbol{x},\boldsymbol{H}}\left[\sum_{\boldsymbol{r}} P(\boldsymbol{r}|\boldsymbol{x},\boldsymbol{H})\ln\frac{P(\boldsymbol{r}|\boldsymbol{x},\boldsymbol{H})}{P(\boldsymbol{r}|\boldsymbol{H})}\right], \tag{7}$$

with $P(\boldsymbol{r}|\boldsymbol{H}) = \mathrm{E}_{\boldsymbol{x}}[P(\boldsymbol{r}|\boldsymbol{x},\boldsymbol{H})]$ and $\mathrm{E}_{\boldsymbol{x}}[\cdot]$ is the expectation taken with respect to $\boldsymbol{x}$. For large N, the computation of the mutual information has intractable complexity due to the summation over all possible $\boldsymbol{r}$, except for low dimensional outputs (see [28] for the single output case), which is not relevant for the massive MIMO case. Therefore, we resort to a low SNR approximation to perform the analysis on the achievable rates.

A. Second-Order Expansion of the Mutual Information With 1-Bit Receivers for Deterministic Channels

In this section, we will elaborate on the second-order expansion of the input-output mutual information (7) of the considered system in Fig. 2 for a given channel matrix $\boldsymbol{H} = \tilde{\boldsymbol{H}}$ as the signal-to-noise ratio goes to zero.

Theorem 2: Consider the one-bit quantized MIMO system in Fig. 2 under a zero-mean input distribution $p(\boldsymbol{x})$ with covariance matrix $\boldsymbol{C}_{\boldsymbol{x}}$, satisfying $p(\boldsymbol{x}) = p(\mathrm{j}\boldsymbol{x})$, $\forall \boldsymbol{x} \in \mathbb{C}^M$ (zero-mean proper complex distribution)[1] and $\mathrm{E}_{\boldsymbol{x}}[\left\|\tilde{\boldsymbol{H}}\boldsymbol{x}\right\|_4^{4+\alpha}] < \gamma$ for some finite constants $\alpha, \gamma > 0$. Then, to the second order, the mutual information (in nats) between the inputs and the quantized outputs for a particular channel matrix is given by:

$$\begin{aligned} I(\boldsymbol{x};\boldsymbol{r}|\boldsymbol{H}=\tilde{\boldsymbol{H}}) &= \frac{2}{\pi}\mathrm{tr}(\tilde{\boldsymbol{H}}\boldsymbol{C}_{\boldsymbol{x}}\tilde{\boldsymbol{H}}^{\mathrm{H}})\frac{1}{\sigma_\eta^2} - \Big[\frac{2}{\pi^2}\mathrm{tr}((\text{nondiag}(\tilde{\boldsymbol{H}}\boldsymbol{C}_{\boldsymbol{x}}\tilde{\boldsymbol{H}}^{\mathrm{H}}))^2) \\ &\quad + \frac{4}{3\pi}(1-\frac{1}{\pi})\mathrm{E}_{\boldsymbol{x}}[\left\|\tilde{\boldsymbol{H}}\boldsymbol{x}\right\|_4^4]\Big]\frac{1}{\sigma_\eta^4} + \Delta I(\boldsymbol{x};\boldsymbol{r}|\boldsymbol{H}=\tilde{\boldsymbol{H}}), \end{aligned} \tag{8}$$

where $\|\boldsymbol{a}\|_4^4 = \sum_{i,c} a_{i,c}^4$, and the remainder term $\Delta I(\boldsymbol{x};\boldsymbol{r}|\boldsymbol{H}=\tilde{\boldsymbol{H}})$ is $o(\frac{1}{\sigma_\eta^4})$..

[1]This restriction is simply justified by symmetry considerations.

Authorized licensed use limited to: Access paid by The UC Irvine Libraries. Downloaded on May 08,2021 at 22:45:13 UTC from IEEE Xplore. Restrictions apply.

Proof: We start with the definition of the mutual information [58]

$$\begin{aligned} I(\boldsymbol{x};\boldsymbol{r}|\boldsymbol{H}=\tilde{\boldsymbol{H}}) &= H(\boldsymbol{r}|\boldsymbol{H}=\tilde{\boldsymbol{H}}) - H(\boldsymbol{r}|\boldsymbol{x},\boldsymbol{H}=\tilde{\boldsymbol{H}}) \\ &= H(\mathrm{sign}(\boldsymbol{H}\boldsymbol{x}+\boldsymbol{\eta})|\boldsymbol{H}=\tilde{\boldsymbol{H}}) \\ &\quad - H(\mathrm{sign}(\boldsymbol{H}\boldsymbol{x}+\boldsymbol{\eta})|\boldsymbol{x},\boldsymbol{H}=\tilde{\boldsymbol{H}}), \end{aligned} \tag{9}$$

then we use Corollary 1 and Corollary 2 with $\varepsilon = \frac{1}{\sigma_\eta}$ and $g(\boldsymbol{x}) = \tilde{\boldsymbol{H}}\boldsymbol{x}$ to get the following asymptotic expression:

$$\begin{aligned} &I(\boldsymbol{x};\boldsymbol{r}|\boldsymbol{H}=\tilde{\boldsymbol{H}}) \\ &= 2N\ln 2 - \frac{2}{\pi}\frac{1}{\sigma_\eta^2}\left\|\mathrm{E}[\tilde{\boldsymbol{H}}\boldsymbol{x}]\right\|_2^2 \\ &\quad - \frac{1}{\sigma_\eta^4}\left(\frac{2}{\pi^2}\mathrm{tr}\left((\mathrm{nondiag}(\boldsymbol{C}_{\tilde{\boldsymbol{H}}\boldsymbol{x}}))^2\right)\right. \\ &\quad - \frac{4}{3\pi}\left\|\mathrm{E}[\tilde{\boldsymbol{H}}\boldsymbol{x}]\circ\mathrm{E}[\tilde{\boldsymbol{H}}\boldsymbol{x}\circ\tilde{\boldsymbol{H}}\boldsymbol{x}\circ\tilde{\boldsymbol{H}}\boldsymbol{x}]\right\|_1^1 \\ &\quad \left. + \frac{4}{3\pi^2}\left\|\mathrm{E}[\tilde{\boldsymbol{H}}\boldsymbol{x}]\right\|_4^4\right) - 2N\ln 2 + \frac{2}{\pi}\frac{1}{\sigma_\eta^2}\mathrm{E}_{\boldsymbol{x}}[\left\|\mathrm{E}[\tilde{\boldsymbol{H}}\boldsymbol{x}|\boldsymbol{x}]\right\|_2^2] \\ &\quad + \frac{1}{\sigma_\eta^4}\mathrm{E}_{\boldsymbol{x}}\left[\frac{2}{\pi^2}\mathrm{tr}\left(\left(\mathrm{nondiag}(\boldsymbol{C}_{\tilde{\boldsymbol{H}}\boldsymbol{x}|\boldsymbol{x}})\right)^2\right)\right. \\ &\quad - \frac{4}{3\pi}\left\|\mathrm{E}[\tilde{\boldsymbol{H}}\boldsymbol{x}|\boldsymbol{x}]\circ\mathrm{E}[\tilde{\boldsymbol{H}}\boldsymbol{x}\circ\tilde{\boldsymbol{H}}\boldsymbol{x}\circ\tilde{\boldsymbol{H}}\boldsymbol{x}|\boldsymbol{x}]\right\|_1^1 \\ &\quad \left. + \frac{4}{3\pi^2}\left\|\mathrm{E}[\tilde{\boldsymbol{H}}\boldsymbol{x}|\boldsymbol{x}]\right\|_4^4\right] + \Delta I(\boldsymbol{x};\boldsymbol{r}|\boldsymbol{H}=\tilde{\boldsymbol{H}}) \\ &= \frac{2}{\pi}\frac{1}{\sigma_\eta^2}\mathrm{E}\left\|[\tilde{\boldsymbol{H}}(\boldsymbol{x}-\mathrm{E}[\boldsymbol{x}])]\right\|_2^2 \\ &\quad - \frac{1}{\sigma_\eta^4}\left(\frac{2}{\pi^2}\mathrm{tr}\left(\left(\mathrm{nondiag}(\tilde{\boldsymbol{H}}\boldsymbol{C}_{\boldsymbol{x}}\tilde{\boldsymbol{H}}^{\mathrm{H}})\right)^2\right)\right. \\ &\quad - \frac{4}{3\pi}\left\|\mathrm{E}[\tilde{\boldsymbol{H}}\boldsymbol{x}]\circ\mathrm{E}[\tilde{\boldsymbol{H}}\boldsymbol{x}\circ\tilde{\boldsymbol{H}}\boldsymbol{x}\circ\tilde{\boldsymbol{H}}\boldsymbol{x}]\right\|_1^1 + \frac{4}{3\pi^2}\mathrm{E}[\left\|\tilde{\boldsymbol{H}}\mathrm{E}[\boldsymbol{x}]\right\|_4^4] \\ &\quad \left. + \frac{4}{3\pi}\mathrm{E}[\left\|\tilde{\boldsymbol{H}}\boldsymbol{x}\right\|_4^4] - \frac{4}{3\pi^2}\mathrm{E}[\left\|\tilde{\boldsymbol{H}}\boldsymbol{x}\right\|_4^4]\right) + \Delta I(\boldsymbol{x};\boldsymbol{r}|\boldsymbol{H}=\tilde{\boldsymbol{H}}). \end{aligned} \tag{10}$$

In the case that the distribution is zero-mean $\mathrm{E}[\boldsymbol{x}] = \boldsymbol{0}$, we end up exactly with the formula stated by the theorem. Again, the condition $\mathrm{E}_{\boldsymbol{x}}[\left\|\tilde{\boldsymbol{H}}\boldsymbol{x}\right\|_4^{4+\alpha}] < \gamma$ for some finite constants $\alpha, \gamma > 0$ ensures that the remainder term

$$|\Delta I(\boldsymbol{x};\boldsymbol{r}|\boldsymbol{H}=\tilde{\boldsymbol{H}})| = \mathrm{E}_{\boldsymbol{x}}[o(\left\|\tilde{\boldsymbol{H}}\boldsymbol{x}\right\|_4^4 \frac{1}{\sigma_\eta^4})] \leq \gamma^{\frac{4+\alpha'}{4+\alpha}}\varepsilon^{4+\alpha'},$$

for some $\alpha' \in]0, \alpha]$ and is therefore $o(\frac{1}{\sigma_\eta^4})$, which follows the explanation given in (109), Appendix A. □

For comparison, we use the results of Prelov and Verdú [51] to express the mutual information between the input $\boldsymbol{x}$ and the unquantized output $\boldsymbol{y}$ with the same input distribution as in Theorem 2:

$$\begin{aligned} &I(\boldsymbol{x};\boldsymbol{y}|\boldsymbol{H}=\tilde{\boldsymbol{H}}) \\ &= \mathrm{tr}(\tilde{\boldsymbol{H}}\boldsymbol{C}_{\boldsymbol{x}}\tilde{\boldsymbol{H}}^{\mathrm{H}})\frac{1}{\sigma_\eta^2} - \frac{\mathrm{tr}((\tilde{\boldsymbol{H}}\boldsymbol{C}_{\boldsymbol{x}}\tilde{\boldsymbol{H}}^{\mathrm{H}})^2)}{2}\frac{1}{\sigma_\eta^4} + o(\frac{1}{\sigma_\eta^4}). \end{aligned} \tag{11}$$

While the mutual information for the unquantized channel in (11), up to the second order, depends only on the input covariance matrix, in the quantized case (8) it also depends on the fourth order statistics of $\boldsymbol{x}$ (the fourth mixed moments of its components).

Now, using (8) and (11), we deduce the mutual information penalty in the low SNR (or large dimension) regime incurred by quantization for non-zero finite channels

$$\lim_{\frac{1}{\sigma_\eta^2}\to 0}\frac{I(\boldsymbol{x};\boldsymbol{r}|\boldsymbol{H}=\tilde{\boldsymbol{H}})}{I(\boldsymbol{x};\boldsymbol{y}|\boldsymbol{H}=\tilde{\boldsymbol{H}})} = \frac{2}{\pi}, \tag{12}$$

which is independent of the channel and the chosen distribution.

In order to apply the ratio of the low-SNR maximum achievable rate of the 1-bit system to the ideal capacity, one must characterize the capacity-achieving distribution and check the validity of the condition $\mathrm{E}_{\boldsymbol{x}}[\left\|\tilde{\boldsymbol{H}}\boldsymbol{x}\right\|_4^{4+\alpha}] < \gamma$ to apply the asymptotic analysis. In [19], it is shown that the capacity-achieving input distribution of the AWGN channel with finite resolution ADCs is, under an average power constraint, bounded and discrete. As a generalization, we show in Appendix B that the capacity-achieving distribution of the 1-bit MIMO channel is bounded and therefore the conditions of Theorem 2 are also valid for the 1-bit channel capacity.

Theorem 3: The capacity-achieving input distribution of the coherent one-bit quantized MIMO system in Fig. 2 under an average power constraint has bounded support.

Proof: See Appendix B. □

Bounded support is a very suitable property motivated by practical limitations. By contrast, the ideal case with infinite resolution requires a Gaussian input distribution with unbounded support. Due to the boundedness of the capacity-achieving distribution for the 1-bit case, the second-order expansion (8) holds also for the capacity. Therefore, we obtain the same ratio (12) for the capacity, i.e., the supremum of the mutual information

$$\lim_{\frac{1}{\sigma_\eta^2}\to 0}\frac{C_{1\text{-bit}}}{C_{\infty\text{-bit}}} = \frac{2}{\pi}. \tag{13}$$

These results can also be obtained based on the pseudo-quantization noise model [15], [25] and it generalizes the result known for the AWGN channel [49].

For a larger number of antennas, the summation in (7) may be intractable. In this case, the second-order approximation in (8) is advantageous at low SNR to overcome the high complexity of the exact formula.

B. Capacity With Independent-Component Inputs for Deterministic Channels

Lacking knowledge of the channel, the transmitter assigns the power evenly over the components $x_{i,c}$ of the input vector $\boldsymbol{x}$, i.e., $\mathrm{E}[x_{i,c}^2] = \frac{P_{\mathrm{Tr}}}{2M}$, in order to achieve good performance on average. Furthermore, let us assume these components to be independent of each other (e. g. multi-streaming scenario).[2]

[2]Clearly, this is not necessarily the capacity-achieving strategy.

Authorized licensed use limited to: Access paid by The UC Irvine Libraries. Downloaded on May 08,2021 at 22:45:13 UTC from IEEE Xplore. Restrictions apply.

Thus, the probability density function of the input vector x is $p(x) = \prod_{i,c} p_{i,c}(x_{i,c})$.[3] Now, with

$$[\tilde{H}x]_{i,R} = \left(\sum_j [\tilde{h}_{i,j,R}x_{j,R} - \tilde{h}_{i,j,I}x_{j,I}]\right), \quad (14)$$

$$\mu_{j,c} = \frac{\mathrm{E}[x_{j,c}^4]}{\mathrm{E}[x_{j,c}^2]^2} = \frac{4M^2}{P_{\mathrm{Tr}}^2}\mathrm{E}[x_{j,c}^4], \quad (15)$$

and the *kurtosis* of the random component $x_{j,c}$ defined as

$$\kappa_{j,c} = \mu_{j,c} - 3, \quad (16)$$

we get

$$\begin{aligned}\mathrm{E}_x[([\tilde{H}x]_{i,R})^4] &= \frac{P_{\mathrm{Tr}}^2}{4M^2}\left(3\sum_{\substack{j,c,j',c'\\(j,c)\neq(j',c')}}\tilde{h}_{i,j,c}^2\tilde{h}_{i,j',c'}^2 + \sum_{j,c}\mu_{j,c}\tilde{h}_{i,j,c}^4\right)\\ &= \frac{P_{\mathrm{Tr}}^2}{4M^2}\left(3\left(\left[\tilde{H}\tilde{H}^{\mathrm{H}}\right]_{i,i}\right)^2 + \sum_{j,c}\kappa_{j,c}\tilde{h}_{i,j,c}^4\right).\end{aligned} \quad (17)$$

Similar results hold for the other components of the vector $\tilde{H}x$. Plugging this result and $C_x = \frac{P_{\mathrm{Tr}}}{M}\mathbf{I}$ into (8), we obtain an expression for the mutual information with independent-component inputs and $C_x = \frac{P_{\mathrm{Tr}}}{M}\mathbf{I}$ up to second order:

$$\begin{aligned}I^{\mathrm{ind}}(x;r|H=\tilde{H}) &= \frac{2}{\pi}\mathrm{tr}(\tilde{H}\tilde{H}^{\mathrm{H}})\frac{P_{\mathrm{Tr}}}{M\sigma_\eta^2}\\ &-\left[\frac{2}{3\pi}(1-\frac{1}{\pi})\left(3\ \mathrm{tr}((\mathrm{diag}(\tilde{H}\tilde{H}^{\mathrm{H}}))^2) + \sum_{i,j,c}\kappa_{j,c}\tilde{h}_{i,j,c}^4\right)\right.\\ &\left.+\frac{2}{\pi^2}\mathrm{tr}((\mathrm{nondiag}(\tilde{H}\tilde{H}^{\mathrm{H}}))^2)\right]\left(\frac{P_{\mathrm{Tr}}}{M\sigma_\eta^2}\right)^2 + o(1/\sigma_\eta^4).\end{aligned} \quad (18)$$

Now, we state a theorem on the structure of the near-optimal input distribution under these assumptions.

Theorem 4: To second order, QPSK signals are capacity-achieving among all signal distributions with independent components. The achieved capacity up to second order is

$$\begin{aligned}C_{\text{1-bit}} &= \frac{2}{\pi}\mathrm{tr}(\tilde{H}\tilde{H}^{\mathrm{H}})\frac{P_{\mathrm{Tr}}}{M\sigma_\eta^2}\\ &-\left[\frac{2}{3\pi}(1-\frac{1}{\pi})\left(3\ \mathrm{tr}((\mathrm{diag}(\tilde{H}\tilde{H}^{\mathrm{H}}))^2) - 2\sum_{i,j,c}\tilde{h}_{i,j,c}^4\right)\right.\\ &\left.+\frac{2}{\pi^2}\mathrm{tr}((\mathrm{nondiag}(\tilde{H}\tilde{H}^{\mathrm{H}}))^2)\right]\left(\frac{P_{\mathrm{Tr}}}{M\sigma_\eta^2}\right)^2 + o(1/\sigma_\eta^4).\end{aligned} \quad (19)$$

Proof: Since $\mathrm{E}[x_{i,c}^4] \geq \mathrm{E}[x_{i,c}^2]^2$, we have $\kappa_{i,c} = \frac{\mathrm{E}[x_{i,c}^4]}{\mathrm{E}[x_{i,c}^2]^2} - 3 \geq -2, \forall i, c$. Obviously, the QPSK distribution is the unique distribution with independent-component inputs that can achieve the minimum value -2 for all indices $\{i, c\}$ simultaneously, i.e., $\kappa_{i,c} = \kappa_{\mathrm{QPSK}} = -2\ \forall i, c$, and thus maximize $I^{\mathrm{ind}}(x; r|H = \tilde{H})$ in (18) up to second order. □

[3]Note that $p_{i,c}(x_{i,c})$ has to be an even function and $p_{i,R}(x_{i,R}) = p_{i,I}(x_{i,I})\ \forall i$, due to the symmetry (see Theorem 2) and convexity of the mutual information.

C. Ergodic Capacity Under i.i.d. Rayleigh Fading Conditions

Here we assume the channel H to be ergodic with i.i.d. Gaussian components $h_{i,j} \sim \mathcal{CN}(0, 1)$. The ergodic capacity can be written as

$$C_{\text{1-bit}}^{\mathrm{erg}} = \mathrm{E}_H[C_{\text{1-bit}}]. \quad (20)$$

We apply the expectation over H using the second order expansion of $C_{\text{1-bit}}$ in (19). By expanding the following expressions and taking the expectation over the i.i.d. channel coefficients, we have

$$\begin{aligned}\mathrm{E}_H\left[\mathrm{tr}(HC_xH^{\mathrm{H}})\right] &= N\mathrm{tr}(C_x)\\ \mathrm{E}_H\left[\mathrm{tr}\left((\mathrm{nondiag}(HC_xH^{\mathrm{H}}))^2\right)\right] &= N(N-1)\mathrm{tr}(C_x^2)\\ \mathrm{E}_H\left[\|Hx\|_4^4\right] &= \frac{3}{2}N\mathrm{E}_x\left[\|x\|_2^4\right].\end{aligned}$$

The ergodic mutual information over an i.i.d. channel can be obtained as

$$\begin{aligned}I(x;r|H) &= N\mathrm{tr}(C_x)\frac{2}{\pi}\frac{1}{\sigma_\eta^2}\\ &-\frac{N}{2}\left((N-1)\mathrm{tr}(C_x^2) + (\pi-1)\mathrm{E}_x\left[\|x\|_2^4\right]\right)\left(\frac{2}{\pi}\frac{1}{\sigma_\eta^2}\right)^2\\ &+o(1/\sigma_\eta^4).\end{aligned} \quad (21)$$

Next, we characterize the capacity-achieving distribution up to second order in the SNR.

Theorem 5: The ergodic capacity of the 1-bit quantized i.i.d. MIMO channel is achieved asymptotically at low SNR by QPSK signals and reads as

$$C_{\text{1-bit}}^{\mathrm{erg}} = N\frac{2}{\pi}\frac{P_{\mathrm{Tr}}}{\sigma_\eta^2} - \frac{N(N+(\pi-1)M-1)}{2M}\left(\frac{2}{\pi}\frac{P_{\mathrm{Tr}}}{\sigma_\eta^2}\right)^2 + o(1/\sigma_\eta^4). \quad (22)$$

Proof: Since $\mathrm{tr}(C_x^2)/M \geq (\mathrm{tr}(C_x)/M)^2 = P_{\mathrm{Tr}}^2/M^2$ with equality if $C_x = \frac{P_{\mathrm{Tr}}}{M}\mathbf{I}$, and $\mathrm{E}_x\left[\|x\|_2^4\right] \geq \left(\mathrm{E}_x\left[\|x\|_2^2\right]\right)^2 = P_{\mathrm{Tr}}^2$ with equality if the input has a constant norm of 1, the ergodic capacity is achieved by a constant-norm uncorrelated input ($C_x = \frac{P_{\mathrm{Tr}}}{M}\mathbf{I}$ and $\|x\|_2^2 = P_{\mathrm{Tr}}$), which can be obtained for instance by QPSK signals Finally, using (19) we obtain the second-order expression for the ergodic capacity of one-bit quantized Rayleigh fading channels for the QPSK case. □

Fig. 3 illustrates the ergodic mutual information for a randomly generated 4×4 channel with entries drawn from $h_{i,j} \sim \mathcal{CN}(0, 1)$, QPSK signaling and total power $\mathrm{tr}(C_x) = P_{\mathrm{Tr}} = \mathrm{SNR}\cdot\sigma_\eta^2$, computed exactly using (7), and also its first and second-order approximations from (22). For comparison, the mutual information without quantization (using an i.i.d. Gaussian input) is also plotted. Fig. 3 shows that the ratio $\frac{2}{\pi}$ holds for low to moderate $\mathrm{SNR} = \frac{P_{\mathrm{Tr}}}{\sigma_\eta^2}$.

Authorized licensed use limited to: Access paid by The UC Irvine Libraries. Downloaded on May 08,2021 at 22:45:13 UTC from IEEE Xplore. Restrictions apply.

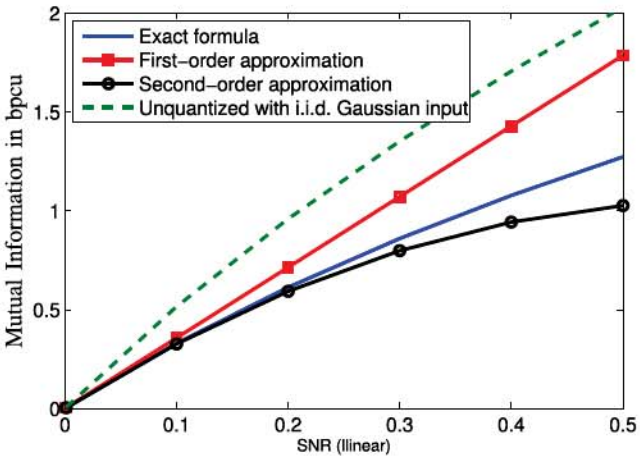

Fig. 3. Mutual information of a 1-bit quantized 4×4 QPSK MIMO system and its first and second-order approximations. The channel is assumed to be i.i.d. Rayleigh fading with unit variance. For comparison the capacity without quantization is also plotted.

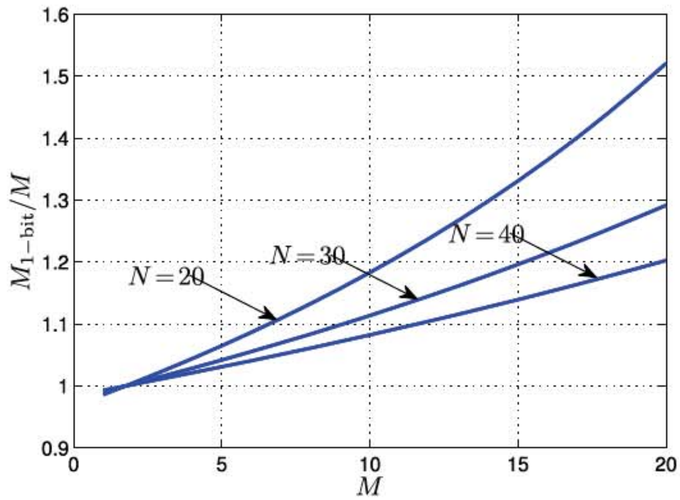

Fig. 4. Required $M_{1-\mathrm{bit}}/M$ to achieve ideal ergodic capacity up to the second order.

Compared to the ergodic capacity in the unquantized case achieved by i.i.d. Gaussian inputs (or even by QPSK up to the second order) [50]

$$C^{\mathrm{erg}}=N\cdot\frac{P_{\mathrm{Tr}}}{\sigma_\eta^2}-\frac{N(N+M)}{2M}\left(\frac{P_{\mathrm{Tr}}}{\sigma_\eta^2}\right)^2+o(1/\sigma_\eta^4),\qquad(23)$$

the ergodic capacity of one-bit quantized MIMO under QPSK $C^{\mathrm{erg}}_{\text{1-bit}}$ incorporates a power penalty of $\frac{\pi}{2}$ (1.96 dB), when considering only the linear term that characterizes the capacity in the limit of infinite bandwidth.

On the other hand, the second-order term quantifies the convergence of the capacity function to the low SNR limit, i.e. the first-order term, by reducing the power or increasing the bandwidth [50]. Since the second order derivative more negatively affects the capacity in the quantized case, i.e., the ratio of the second order terms in (22) and (23) for equal first order terms is larger than one

$$1<\frac{N+(\pi-1)M-1}{N+M}<\pi-1,\qquad(24)$$

it can be concluded that the low-SNR capacity of the quantized channel converges to the asymptotic capacity at a slower rate than the unquantized channel. Nevertheless, for $M=1$ or $M\ll N$ (massive MIMO uplink scenario), this difference in the convergence behavior vanishes almost completely, since both second-order expansions (22) and (23) become nearly the same up to the factor $2/\pi$ in SNR.

In addition, the ergodic capacity of the quantized channel $C^{\mathrm{erg}}_{\text{1-bit}}$ in (22) increases linearly with the number of receive antennas N while the number of transmit antennas M only appears in the second-order term, which holds also for C^{erg}. For the special case of one receive antenna, $N=1$, $C^{\mathrm{erg}}_{\text{1-bit}}$ does not depend on the number of transmit antennas M up to the second order, contrary to C^{erg}. On the other hand, if one would achieve, up to the second order, the same ergodic capacity at the same power with one-bit receivers as in the ideal case by adjusting the number of receive and transmit antennas, i.e.,

$$N\cdot\frac{P_{\mathrm{Tr}}}{\sigma_\eta^2}-\frac{N(N+M)}{2M}\left(\frac{P_{\mathrm{Tr}}}{\sigma_\eta^2}\right)^2=N_{1-\mathrm{bit}}\frac{2}{\pi}\frac{P_{\mathrm{Tr}}}{\sigma_\eta^2}-\frac{N_{1-\mathrm{bit}}(N_{1-\mathrm{bit}}+(\pi-1)M_{1-\mathrm{bit}}-1)}{2M_{1-\mathrm{bit}}}\left(\frac{2}{\pi}\frac{P_{\mathrm{Tr}}}{\sigma_\eta^2}\right)^2,\qquad(25)$$

then we can deduce by equating coefficients that

$$N_{1-\mathrm{bit}}=\frac{\pi}{2}N,\qquad M_{1-\mathrm{bit}}=M\frac{\pi N-2}{\pi N-(\pi-2)M}.\qquad(26)$$

The one-bit receive dimension has to be increased by $\pi/2$, while the behavior for the number of transmit antennas is shown in Fig. 4. Clearly, when $N\gg M$, which corresponds to a typical massive MIMO uplink scenario, we have $M_{1-\mathrm{bit}}\approx M$. This means that, at the transmitter (or user) side, there is no need to increase the number of antennas up to the second order in SNR, showing that the total increase of dimensions is moderate.

V. Mutual Information and Capacity With Statistical CSI and 1-Bit Receivers

We reconsider now the extreme case of 1-bit quantized communications over MIMO Rayleigh-fading channels but assuming that only the statistics of the channel are known at the receiver. Later, we will also treat the achievable rate for the SISO channel case for the whole SNR range.

Generally, the mutual information (in nats/channel use) between the channel input and the quantized output in Fig. 2 with statistical CSI reads as [58]

$$I(\boldsymbol{x};\boldsymbol{r})=H(\boldsymbol{r})-H(\boldsymbol{r}|\boldsymbol{x})=\mathrm{E}_{\boldsymbol{x}}\left[\sum_{\boldsymbol{r}}P(\boldsymbol{r}|\boldsymbol{x})\ln\frac{P(\boldsymbol{r}|\boldsymbol{x})}{P(\boldsymbol{r})}\right],\qquad(27)$$

Authorized licensed use limited to: Access paid by The UC Irvine Libraries. Downloaded on May 08,2021 at 22:45:13 UTC from IEEE Xplore. Restrictions apply.

where $P(r) = \mathrm{E}_{\boldsymbol{x}}[P(\boldsymbol{r}|\boldsymbol{x})]$ and $H(\cdot)$ and $H(\cdot|\cdot)$ represent the entropy and the conditional entropy, respectively. If the channel is Gaussian distributed with zero mean, then given the input x, the unquantized output y is zero-mean complex Gaussian with covariance $\mathrm{E}[\boldsymbol{y}\boldsymbol{y}^{\mathrm{H}}|\boldsymbol{x}] = \sigma_\eta^2 \cdot \mathbf{I}_N + \mathrm{E}_{\boldsymbol{H}}[\boldsymbol{H}\boldsymbol{x}\boldsymbol{x}^{\mathrm{H}}\boldsymbol{H}^{\mathrm{H}}]$, and thus we have

$$p(\boldsymbol{y}|\boldsymbol{x}) = \frac{\exp(-\boldsymbol{y}^{\mathrm{H}}(\sigma_\eta^2\mathbf{I}_N + \mathrm{E}_{\boldsymbol{H}}[\boldsymbol{H}\boldsymbol{x}\boldsymbol{x}^{\mathrm{H}}\boldsymbol{H}^{\mathrm{H}}])^{-1}\boldsymbol{y})}{\pi^N \left|\sigma_\eta^2\mathbf{I}_N + \mathrm{E}_{\boldsymbol{H}}[\boldsymbol{H}\boldsymbol{x}\boldsymbol{x}^{\mathrm{H}}\boldsymbol{H}^{\mathrm{H}}]\right|}. \quad (28)$$

Thus, we can express the conditional probability of the quantized output as

$$\begin{aligned} P(\boldsymbol{r}|\boldsymbol{x}) &= \int_0^\infty \!\!\cdots\! \int_0^\infty p(\boldsymbol{y}\circ\boldsymbol{r}|\boldsymbol{x})\mathrm{d}\boldsymbol{r} \\ &= \int_0^\infty \!\!\cdots\! \int_0^\infty \\ &\frac{\exp(-(\boldsymbol{y}\circ\boldsymbol{r})^{\mathrm{H}}(\sigma_\eta^2\cdot\mathbf{I}_N + \mathrm{E}[\boldsymbol{H}\boldsymbol{x}\boldsymbol{x}^{\mathrm{H}}\boldsymbol{H}^{\mathrm{H}}])^{-1}(\boldsymbol{y}\circ\boldsymbol{r}))}{\pi^N\left|\sigma_\eta^2\cdot\mathbf{I}_N + \mathrm{E}[\boldsymbol{H}\boldsymbol{x}\boldsymbol{x}^{\mathrm{H}}\boldsymbol{H}^{\mathrm{H}}]\right|}\mathrm{d}\boldsymbol{y}, \end{aligned} \quad (29)$$

where the integration is performed over the positive orthant of the complex hyperplane.

The evaluation of this multiple integral is in general intractable. Thus, we consider first a simple lower bound involving the mutual information under perfect channel state information at the receiver, which turns out to be tight in some cases as shown later. The lower bound is obtained by the chain rule and the non-negativity of the mutual information:

$$\begin{aligned} I(\boldsymbol{x};\boldsymbol{r}) &= \mathrm{E}_{\boldsymbol{x},\boldsymbol{H}}\left[\sum_{\boldsymbol{r}} P(\boldsymbol{r}|\boldsymbol{x},\boldsymbol{H})\ln\frac{\mathrm{E}_{\boldsymbol{H}}[P(\boldsymbol{r}|\boldsymbol{x},\boldsymbol{H})]}{\mathrm{E}_{\boldsymbol{x},\boldsymbol{H}}[P(\boldsymbol{r}|\boldsymbol{x},\boldsymbol{H})]}\right] \\ &= I(\boldsymbol{H};\boldsymbol{r}) + I(\boldsymbol{x};\boldsymbol{r}|\boldsymbol{H}) - I(\boldsymbol{H};\boldsymbol{r}|\boldsymbol{x}) \\ &\geq I(\boldsymbol{x};\boldsymbol{r}|\boldsymbol{H}) - I(\boldsymbol{H};\boldsymbol{r}|\boldsymbol{x}) \\ &= \mathrm{E}_{\boldsymbol{x},\boldsymbol{H}}\left[\sum_{\boldsymbol{r}} P(\boldsymbol{r}|\boldsymbol{x},\boldsymbol{H})\ln\frac{\mathrm{E}_{\boldsymbol{H}}[P(\boldsymbol{r}|\boldsymbol{x},\boldsymbol{H})]}{\mathrm{E}_{\boldsymbol{x}}[P(\boldsymbol{r}|\boldsymbol{x},\boldsymbol{H})]}\right] \\ &= \mathrm{E}_{\boldsymbol{x},\boldsymbol{H}}\left[\sum_{\boldsymbol{r}} P(\boldsymbol{r}|\boldsymbol{x},\boldsymbol{H})\ln\frac{P(\boldsymbol{r}|\boldsymbol{x})}{P(\boldsymbol{r}|\boldsymbol{H})}\right]. \end{aligned} \quad (30)$$

On the other hand, an upper bound is given by the coherent assumption (channel perfectly known at the receiver)

$$I(\boldsymbol{x};\boldsymbol{r}) \leq \mathrm{E}_{\boldsymbol{x},\boldsymbol{H}}\left[\sum_{\boldsymbol{r}} P(\boldsymbol{r}|\boldsymbol{x},\boldsymbol{H})\cdot\ln\frac{P(\boldsymbol{r}|\boldsymbol{x},\boldsymbol{H})}{P(\boldsymbol{r}|\boldsymbol{H})}\right], \quad (31)$$

where we can express each of the conditional probabilities $P(\boldsymbol{r}|\boldsymbol{x},\boldsymbol{H})$ as the product of the conditional probabilities on each receiver dimension, since the real and imaginary components of the receiver noise η are statistically independent with power $\frac{1}{2}$ in each real dimension:

$$\begin{aligned} P(\boldsymbol{r}|\boldsymbol{x},\boldsymbol{H}) &= \prod_{c\in\{R,I\}}\prod_{i=1}^{N} P(r_{i,c}|\boldsymbol{x}) \\ &= \prod_{c\in\{R,I\}}\prod_{i=1}^{N}\Phi\left(r_{i,c}[\boldsymbol{H}\boldsymbol{x}]_{i,c}\sqrt{2\mathrm{SNR}}\right), \end{aligned} \quad (32)$$

where $\Phi(x) = \frac{1}{\sqrt{2\pi}}\int_{-\infty}^{x} e^{-\frac{t^2}{2}}dt$ is the cumulative normal distribution function. Evaluating the lower bound in (30), even numerically, is very difficult, except for some simple cases such as SISO block fading channels, as considered next.

A. The Non-Coherent Block-Rayleigh Fading SISO Case

Here we treat the block-Rayleigh fading SISO case in more detail, where $\boldsymbol{H} = h\cdot\mathbf{I}_T$, $h \sim \mathcal{CN}(0,1)$, and $M = N = T$ is the coherence time. For ease of notation we assume that $\sigma_\eta^2 = 1$, therefore we have without loss of generality $\mathrm{SNR} = \frac{P_{\mathrm{Tr}}}{\sigma_\eta^2} = P_{\mathrm{Tr}}$. The covariance matrix $\mathrm{E}[\boldsymbol{y}\boldsymbol{y}^{\mathrm{H}}|\boldsymbol{x}] = \mathbf{I}_T + \boldsymbol{x}\boldsymbol{x}^{\mathrm{H}}$ is the sum of an identity matrix and a rank one matrix. Then, we obtain the conditional probability of the 1-bit output as

$$\begin{aligned} P(\boldsymbol{r}|\boldsymbol{x}) &= \mathrm{E}_h[P(\boldsymbol{r}|\boldsymbol{x},h)] \\ &= \frac{1}{\pi}\int_{\mathbb{C}} e^{-|h|^2}\prod_{t=1}^{T}\prod_{c\in\{R,I\}}\Phi(\sqrt{2}([hx_t]_c)r_{t,c})\cdot\mathrm{d}h \\ &= \frac{1}{\pi}\int_{\mathbb{C}} e^{-|h|^2}\prod_{t=1}^{T}\Phi(\sqrt{2}\mathrm{Re}(hx_t)r_{t,R})\Phi(\sqrt{2}\mathrm{Im}(hx_t)r_{t,I})\mathrm{d}h \\ &= \frac{1}{2\pi}\int_{-\infty}^{+\infty}\int_{-\infty}^{+\infty} e^{-\frac{u^2+v^2}{2}}\prod_{t=1}^{T}\Phi((x_{t,R}u - x_{t,I}v)r_{t,R}) \\ &\qquad\cdot\Phi((x_{t,R}v + x_{t,I}u)r_{t,I})\mathrm{d}u\mathrm{d}v, \end{aligned} \quad (33)$$

where $\Phi(x) = \frac{1}{\sqrt{2\pi}}\int_{-\infty}^{x} e^{-\frac{t^2}{2}}dt$ is the cumulative normal distribution function. The conditional probability (33) has the following property

$$P(\boldsymbol{r}\circ\boldsymbol{z}|\boldsymbol{x}\circ\boldsymbol{z}) = P(\boldsymbol{r}|\boldsymbol{x}), \forall \boldsymbol{z}\in\{\pm1,\pm\mathrm{j}\}^T. \quad (34)$$

1) Achievable Rate With i.i.d. QPSK for the 1-Bit Block Fading SISO Model: With the invariance property (34), the achievable rate of the one-bit quantized SISO channel with QPSK input in bits per channel use reads as

$$\begin{aligned} \mathcal{R}_{1-\mathrm{bit}}^{\mathrm{QPSK}}(\mathrm{SNR}) &= \frac{1}{T}\frac{1}{4^T}\sum_{\boldsymbol{x}}\sum_{\boldsymbol{r}} P(\boldsymbol{r}|\boldsymbol{x})\log_2(\frac{P(\boldsymbol{r}|\boldsymbol{x})}{P(\boldsymbol{r})}) \\ &= \frac{1}{T}\sum_{\boldsymbol{r}} P(\boldsymbol{r}|\boldsymbol{x}^0)\log_2(4^T P(\boldsymbol{r}|\boldsymbol{x}^0)), \end{aligned} \quad (35)$$

Here, $\boldsymbol{x}$ is drawn from all possible sequences of T equally likely QPSK data symbols, i.e., $x \in \{\sqrt{\mathrm{SNR}}, -\sqrt{\mathrm{SNR}}, \mathrm{j}\sqrt{\mathrm{SNR}}, -\mathrm{j}\sqrt{\mathrm{SNR}}\}^T$ and $\boldsymbol{x}^0$ denotes the constant sequence $x_t^0 = \sqrt{\mathrm{SNR}}, \forall t$. The second equality in (35) follows due to the symmetry of the QPSK constellation and since

$$\begin{aligned} P(\boldsymbol{r}) &= \frac{1}{4^T}\sum_{\boldsymbol{x}} P(\boldsymbol{r}|\boldsymbol{x}) = \frac{1}{4^T}\sum_{\boldsymbol{x}'\in\{\pm1,\pm\mathrm{j}\}} P(\boldsymbol{r}|\boldsymbol{x}'\circ\boldsymbol{x}^0) \\ &\overset{\text{due to (34)}}{=} \frac{1}{4^T}\sum_{\boldsymbol{x}'\in\{\pm1,\pm\mathrm{j}\}} P(\boldsymbol{x}'\circ\boldsymbol{r}|\boldsymbol{x}^0) \\ &= \frac{1}{4^T}\sum_{\boldsymbol{r}'} P(\boldsymbol{r}'|\boldsymbol{x}^0) = \frac{1}{4^T}, \end{aligned} \quad (36)$$

where we used the property $P(\boldsymbol{r}|\boldsymbol{x}\circ\boldsymbol{z}) = P(\boldsymbol{r}\circ\boldsymbol{z}|\boldsymbol{x})$, $\forall \boldsymbol{z}\in\{\pm1,\pm\mathrm{j}\}^{\mathrm{T}}$ according to (34). We note that the rate expression (35) corresponds exactly to its lower bound in (30) due

Authorized licensed use limited to: Access paid by The UC Irvine Libraries. Downloaded on May 08,2021 at 22:45:13 UTC from IEEE Xplore. Restrictions apply.

to the fact that in the i.i.d. QPSK case $P(\boldsymbol{r}|h) = P(\boldsymbol{r}) = 4^{-T}$ and thus $I(h;\boldsymbol{r}) = 0$. Furthermore, we use (33) to get a simpler expression for $P(\boldsymbol{r}|\boldsymbol{x}^0)$ as

$$\begin{aligned} P(\boldsymbol{r}|\boldsymbol{x}^0) =& \frac{1}{2\pi}\int_{-\infty}^{+\infty} e^{-\frac{u^2}{2}}\prod_{t=1}^{T}\Phi(\sqrt{\mathrm{SNR}}r_{t,R}u)\mathrm{d}u \\ &\times \int_{-\infty}^{+\infty} e^{-\frac{v^2}{2}}\prod_{t=1}^{T}\Phi(\sqrt{\mathrm{SNR}}r_{t,I}v)\mathrm{d}v \\ =& P(\mathrm{Re}(\boldsymbol{r})|\boldsymbol{x}^0)\cdot P(\mathrm{Im}(\boldsymbol{r})|\boldsymbol{x}^0). \end{aligned} \quad (37)$$

Then (35) simplifies to

$$\begin{aligned} \mathcal{R}_{1-\mathrm{bit}}^{\mathrm{QPSK}}(\mathrm{SNR}) =& \frac{2}{T}\sum_{t,r_t=\pm 1}\left(\int_{-\infty}^{+\infty}\frac{e^{-\frac{u^2}{2}}}{\sqrt{2\pi}}\prod_{t=1}^{T}\Phi(\sqrt{\mathrm{SNR}}r_t u)\mathrm{d}u\right) \\ &\times \log_2\left(2^T\int_{-\infty}^{+\infty}\frac{e^{-\frac{u^2}{2}}}{\sqrt{2\pi}}\prod_{t=1}^{T}\Phi(\sqrt{\mathrm{SNR}}r_t u)\mathrm{d}u\right) \\ =& \frac{2}{T}\sum_{k=0}^{T}\binom{T}{k}\left(\int_{-\infty}^{+\infty}\frac{e^{-\frac{u^2}{2}}}{\sqrt{2\pi}}\Phi(-\sqrt{\mathrm{SNR}}u)^k\Phi(\sqrt{\mathrm{SNR}}u)^{T-k}\mathrm{d}u\right) \\ &\times \log_2\left(2^T\int_{-\infty}^{+\infty}\frac{e^{-\frac{u^2}{2}}}{\sqrt{2\pi}}\Phi(-\sqrt{\mathrm{SNR}}u)^k\Phi(\sqrt{\mathrm{SNR}}u)^{T-k}\mathrm{d}u\right). \end{aligned} \quad (38)$$

For the special case $T = 2$, we use the following closed form solution from [59] for the integral in (38)

$$\begin{aligned} &\frac{1}{\sqrt{2\pi}}\int_{-\infty}^{+\infty} e^{-\frac{u^2}{2}}\prod_{t=1}^{2}\Phi(\sqrt{\mathrm{SNR}}r_{t,c}u)\mathrm{d}u \\ &= \frac{1}{4}\left[1+\frac{2}{\pi}\arcsin(\frac{\mathrm{SNR}}{1+\mathrm{SNR}})r_{1,c}r_{2,c}\right]. \end{aligned} \quad (39)$$

Thus (38) becomes

$$\begin{aligned} \mathcal{R}_{1-\mathrm{bit},T=2}^{\mathrm{QPSK}}(\mathrm{SNR}) =& \frac{1}{2}\left(1+\frac{2}{\pi}\arcsin(\frac{\mathrm{SNR}}{1+\mathrm{SNR}})\right) \\ &\cdot\log_2\left(1+\frac{2}{\pi}\arcsin(\frac{\mathrm{SNR}}{1+\mathrm{SNR}})\right) \\ &+\frac{1}{2}\left(1-\frac{2}{\pi}\arcsin(\frac{\mathrm{SNR}}{1+\mathrm{SNR}})\right) \\ &\cdot\log_2\left(1-\frac{2}{\pi}\arcsin(\frac{\mathrm{SNR}}{1+\mathrm{SNR}})\right). \end{aligned} \quad (40)$$

And for the case $T = 3$, we substitute using again the corresponding formula from [59]

$$\begin{aligned} &\frac{1}{\sqrt{2\pi}}\int_{-\infty}^{+\infty} e^{-\frac{u^2}{2}}\prod_{t=1}^{3}\Phi(\sqrt{\mathrm{SNR}}r_{t,c}u)\mathrm{d}u \\ &= \frac{1}{8}\left[1+\frac{2}{\pi}\left(\arcsin(\frac{\mathrm{SNR}}{1+\mathrm{SNR}})r_{1,c}r_{2,c}+\arcsin(\frac{\mathrm{SNR}}{1+\mathrm{SNR}})\right.\right. \\ &\left.\left.\cdot r_{1,c}r_{3,c}+\arcsin(\frac{\mathrm{SNR}}{1+\mathrm{SNR}})r_{2,c}r_{3,c}\right)\right] \end{aligned} \quad (41)$$

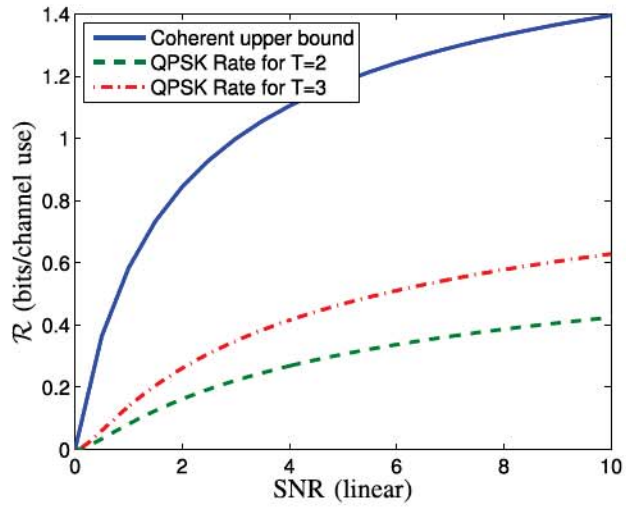

Fig. 5. Achievable rate of the one-bit Rayleigh-fading SISO channel for $T = 2$, $T = 3$, $T = \infty$.

in (38) and we obtain

$$\begin{aligned} \mathcal{R}_{1-\mathrm{bit},T=3}^{\mathrm{QPSK}}(\mathrm{SNR}) =& \frac{1}{3}\left(\frac{1}{2}+\frac{3}{\pi}\arcsin(\frac{\mathrm{SNR}}{1+\mathrm{SNR}})\right) \\ &\cdot\log_2\left(1+\frac{6}{\pi}\arcsin(\frac{\mathrm{SNR}}{1+\mathrm{SNR}})\right) \\ &+\frac{1}{3}\left(\frac{3}{2}-\frac{3}{\pi}\arcsin(\frac{\mathrm{SNR}}{1+\mathrm{SNR}})\right) \\ &\cdot\log_2\left(1-\frac{2}{\pi}\arcsin(\frac{\mathrm{SNR}}{1+\mathrm{SNR}})\right). \end{aligned} \quad (42)$$

A closed form solution for the integral in (37) for $T > 3$ is unknown and only approximations are found in the literature [59].

In Fig. 5, we plot the achievable rate of the one-bit SISO Rayleigh-fading channel per channel use over the SNR for two cases $T = 2$ and $T = 3$. The coherent transmission rate achieved by quantized QPSK, which is an upper bound on our non-coherent capacity (see (31)), is also shown. It is obtained assuming that the receiver knows the channel coefficient h (or T goes to infinity). The average achieved by QPSK over the quantized coherent Rayleigh-fading channel is obtained from (31):

$$\begin{aligned} \mathcal{R}_{1-\mathrm{bit}}^{\mathrm{coh}} &= I(x;r|h) \\ &= \mathrm{E}_h\left[2+\sum_x\sum_y P(r|x,h)\log_2 P(r|x,h)\right] \\ &= 2\left(1-\frac{1}{\sqrt{2\pi}}\int_{-\infty}^{\infty}\mathrm{e}^{-\frac{u^2}{2}}H_b(\Phi(\sqrt{\mathrm{SNR}}\cdot u))\mathrm{d}u\right), \end{aligned} \quad (43)$$

where we have used the binary entropy function $H_b(p) = -p\cdot\log_2 p-(1-p)\cdot\log_2(1-p)$, and we substituted $H(r) = 2$ since all four possible outputs are equiprobable, and

$$P(r|x,h) = \Phi\left(\frac{\mathrm{Re}[y]\mathrm{Re}[hx]}{\sqrt{1/2}}\right)\Phi\left(\frac{\mathrm{Im}[r]\mathrm{Im}[hx]}{\sqrt{1/2}}\right). \quad (44)$$

Authorized licensed use limited to: Access paid by The UC Irvine Libraries. Downloaded on May 08,2021 at 22:45:13 UTC from IEEE Xplore. Restrictions apply.

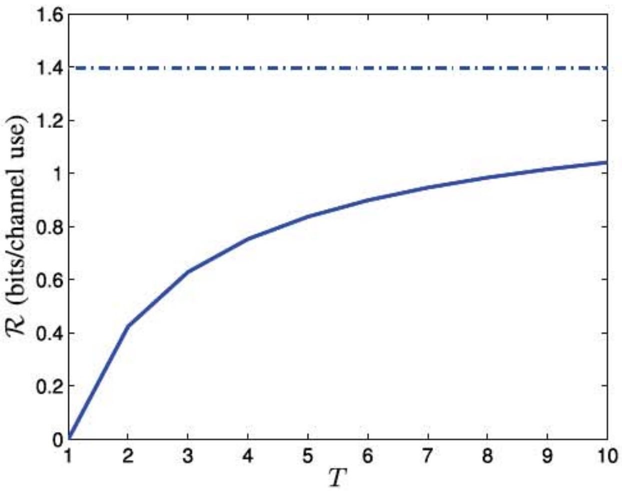

Fig. 6. Achievable rate of the one-bit Rayleigh-fading SISO channel versus coherence interval T for SNR=10dB (dashed curve is for the coherent case $T \to \infty$).

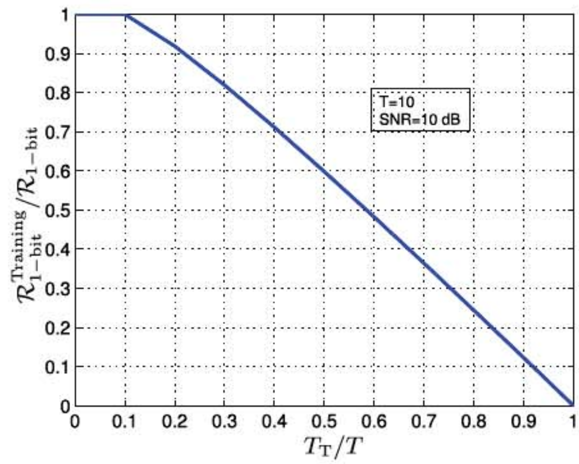

Fig. 7. Achievable rate as a function of the fraction of the coherence time spent on training for $T = 10$ and SNR$=$ 10dB.

In Fig. 6, we plot the normalized achievable rate of the one-bit Rayleigh-fading SISO channel versus coherence interval T for SNR=10dB. The coherent upper bound is also plotted.

2) Training Schemes for the 1-Bit Block Fading Model: Training based schemes are attractive for communication over a priori unknown channels, since the receiver task becomes significantly easier. Therefore, most of the wireless communication standards use part of the transmission block for sending a pilot sequence that is known at the receiver:

$$\boldsymbol{x} = \begin{bmatrix} \boldsymbol{x}_{\mathrm{T}} \\ \boldsymbol{x}_{\mathrm{D}} \end{bmatrix}, \tag{45}$$

where $\boldsymbol{x}_{\mathrm{T}}$ is a fixed known, i.e., deterministic QPSK training vector of length $T_{\mathrm{T}} < T$. This transmit strategy based on the separation of data and training symbols is in general suboptimal from an information theoretical point of view, but is beneficial from a practical point of view. Due to the invariance property (34), the output entropy does not depend on the particular choice of the QPSK training sequence, i.e., the output entropy with a deterministic training vector $\boldsymbol{x}_{1:T_{\mathrm{T}}} = \boldsymbol{x}_{\mathrm{T}}$ is the same as with a random QPSK training vector $\boldsymbol{x}_{1:T_{\mathrm{T}}}$ that is known at the receiver:

$$\begin{aligned} &H(\boldsymbol{r}|\boldsymbol{x}_{1:T_{\mathrm{T}}} = \boldsymbol{x}_{\mathrm{T}}) \\ &= H(\boldsymbol{r}_{1:T_{\mathrm{T}}} \circ \boldsymbol{x}'_{\mathrm{T}}, \boldsymbol{r}_{T_{\mathrm{T}}+1:T_{\mathrm{T}}}|\boldsymbol{x}_{1:T_{\mathrm{T}}} = \boldsymbol{x}_{\mathrm{T}} \circ \boldsymbol{x}'_{\mathrm{T}}), \\ &\qquad\qquad \forall \boldsymbol{x}'_{\mathrm{T}} \in \{\pm 1, \pm \mathrm{j}\}^{T_{\mathrm{T}}} \\ &= \frac{1}{T_{\mathrm{T}}^4} \sum_{\boldsymbol{x}'_{\mathrm{T}} \in \{\pm 1, \pm \mathrm{j}\}^{T_{\mathrm{T}}}} H(\boldsymbol{r}_{1:T_{\mathrm{T}}} \circ \boldsymbol{x}'_{\mathrm{T}}, \boldsymbol{r}_{T_{\mathrm{T}}+1:T_{\mathrm{T}}}|\boldsymbol{x}_{1:T_{\mathrm{T}}} = \boldsymbol{x}_{\mathrm{T}} \circ \boldsymbol{x}'_{\mathrm{T}}) \\ &= \frac{1}{T_{\mathrm{T}}^4} \sum_{\boldsymbol{x}'_{\mathrm{T}} \in \{\pm 1, \pm \mathrm{j}\}^{T_{\mathrm{T}}}} H(\boldsymbol{r}_{1:T_{\mathrm{T}}}, \boldsymbol{r}_{T_{\mathrm{T}}+1:T_{\mathrm{T}}}|\boldsymbol{x}_{1:T_{\mathrm{T}}} = \boldsymbol{x}_{\mathrm{T}} \circ \boldsymbol{x}'_{\mathrm{T}}) \\ &= H(\boldsymbol{r}|\boldsymbol{x}_{1:T_{\mathrm{T}}}). \end{aligned} \tag{46}$$

Consequently, the achievable rate of this scheme with joint processing of data and training can be written as follows:

$$\begin{aligned} \mathcal{R}_{1-\mathrm{bit}}^{\mathrm{Training}} &= \frac{1}{T} H(\boldsymbol{r}|\boldsymbol{x}_{1:T_{\mathrm{T}}}) - \frac{1}{T} H(\boldsymbol{r}|\boldsymbol{x}) \\ &= \frac{1}{T} H(\boldsymbol{r}) - \frac{1}{T} I(\boldsymbol{x}_{1:T_{\mathrm{T}}}; \boldsymbol{r}) - \frac{1}{T} H(\boldsymbol{r}|\boldsymbol{x}) \\ &= \mathcal{R}_{1-\mathrm{bit},T} - \mathcal{R}_{1-\mathrm{bit},T_{\mathrm{T}}}, \end{aligned} \tag{47}$$

where we have used the formula for the mutual information $I(\boldsymbol{x}_{1:T_{\mathrm{T}}};\boldsymbol{r}) = H(\boldsymbol{r}) - H(\boldsymbol{r}|\boldsymbol{x}_{1:T_{\mathrm{T}}}) = T\mathcal{R}_{1-\mathrm{bit},T_{\mathrm{T}}}$. The expression of the capacities with the coherence time can be obtained from (38). In other words, we have taken the difference of the entropy of the quantized output given the training part $\boldsymbol{x}_{1:T_{\mathrm{T}}} = \boldsymbol{x}_{\mathrm{T}}$. In fact, the rate per coherence interval is reduced by an amount that corresponds to the rate (38) with coherence time T_{T}:

$$\begin{aligned} &\mathcal{R}_{1-\mathrm{bit},T_{\mathrm{T}}} = \frac{2}{T} \sum_{k=0}^{T_{\mathrm{T}}} \\ &\binom{T_{\mathrm{T}}}{k} \left(\int_{-\infty}^{+\infty} \frac{e^{-\frac{u^2}{2}}}{\sqrt{2\pi}} \Phi(-\sqrt{\mathrm{SNR}}u)^k \Phi(\sqrt{\mathrm{SNR}}u)^{T_{\mathrm{T}}-k} \mathrm{d}u \right) \\ &\cdot \log_2 \left(2^T \int_{-\infty}^{+\infty} \frac{e^{-\frac{u^2}{2}}}{\sqrt{2\pi}} \Phi(-\sqrt{\mathrm{SNR}}u)^k \Phi(\sqrt{\mathrm{SNR}}u)^{T_{\mathrm{T}}-k} \mathrm{d}u \right). \end{aligned} \tag{48}$$

It is worth mentioning that for the case where we fix one symbol in the input sequence $\boldsymbol{x}$ as a training symbol, we can get the same capacity since $\mathcal{R}_{T_{\mathrm{T}}=1} = 0$. Therefore, in contrast to the unquantized case, a single training symbol for the input sequence $\boldsymbol{x}$ can always be used without any penalty in the channel capacity. Fig. 7 shows the achievable capacity of a SISO channel with a coherence length of $T = 10$ and SNR$=$ 10dB as a function of the training length T_{T}. Again, we observe that only one symbol as training will not reduce the capacity, while the curve then decreases with almost a slope of -1. Therefore, we can see that choosing the training length to be negligible compared with the coherence time is necessary such that the penalty due to the separation of the channel estimation from the data transmission is small enough.

Authorized licensed use limited to: Access paid by The UC Irvine Libraries. Downloaded on May 08,2021 at 22:45:13 UTC from IEEE Xplore. Restrictions apply.

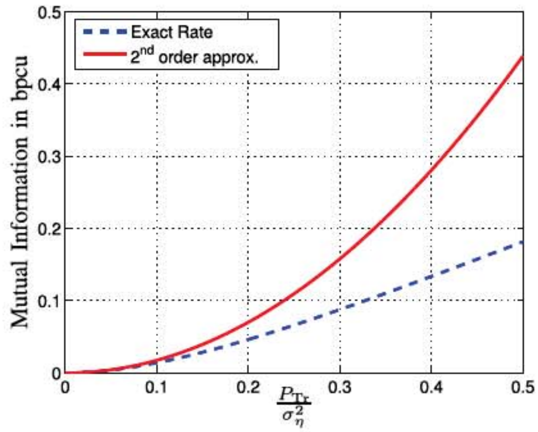

Fig. 8. Mutual information of the one-bit block Rayleigh-faded SISO channel with coherence length 3.

B. Second-Order Expansion of the Mutual Information

In this section, we will consider more general channels and elaborate on the second-order expansion of the input-output mutual information (27) of the considered system in Fig. 2 as the signal-to-noise ratio goes to zero, and where only statistical CSI is available at the receiver. We state the main result and we prove it afterwards.

Theorem 6: Consider the one-bit quantized MIMO system in Fig. 2, where the channel matrix $\boldsymbol{H}$ is zero-mean and circularly distributed, and assume $\mathrm{E}_{\boldsymbol{x},\boldsymbol{H}}[\|\boldsymbol{H}\boldsymbol{x}\|_4^{4+\varepsilon}] < \delta$ is satisfied for some finite constants $\varepsilon, \delta > 0$. Then, to second order, the mutual information (in nats) with statistical CSI between the inputs and the quantized outputs is given by

$$I(\boldsymbol{x};\boldsymbol{r}) = \frac{1}{2}\left(\frac{2}{\pi}\frac{1}{\sigma_\eta^2}\right)^2 \mathrm{tr}\left\{\mathrm{E}\left[(\mathrm{nondiag}(\mathrm{E}[\boldsymbol{H}\boldsymbol{x}\boldsymbol{x}^{\mathrm{H}}\boldsymbol{H}^{\mathrm{H}}|\boldsymbol{x}]))^2\right] - (\mathrm{nondiag}(\mathrm{E}[\boldsymbol{H}\mathrm{E}[\boldsymbol{x}\boldsymbol{x}^{\mathrm{H}}]\boldsymbol{H}^{\mathrm{H}}]))^2\right\} + \underbrace{\Delta I(\boldsymbol{x};\boldsymbol{r})}_{o(\frac{1}{\sigma_\eta^4})}. \quad (49)$$

1) Comments on Theorem 6: As an example, Fig. 8 illustrates the rate expression (42) and the quadratic approximation (49) computed for a block fading SISO model with a coherence interval of 3 symbol periods ($\boldsymbol{H} = h \cdot \mathbf{I}_3$, $h \sim \mathcal{CN}(0,1)$) under QPSK signaling.

A similar result was derived by Prelov and Verdù in [51] for the soft output $\boldsymbol{y}$

$$I(\boldsymbol{x};\boldsymbol{y}) = \frac{1}{2}\frac{1}{\sigma_\eta^4}\mathrm{tr}\left\{\mathrm{E}\left[(\mathrm{E}[\boldsymbol{H}\boldsymbol{x}\boldsymbol{x}^{\mathrm{H}}\boldsymbol{H}^{\mathrm{H}}|\boldsymbol{x}])^2\right] - (\mathrm{E}[\boldsymbol{H}\mathrm{E}[\boldsymbol{x}\boldsymbol{x}^{\mathrm{H}}]\boldsymbol{H}^{\mathrm{H}}])^2\right\} + o(\frac{1}{\sigma_\eta^4}), \quad (50)$$

where we identify a power penalty of $\frac{\pi}{2}$ due to quantization and we see that the diagonal elements of $\mathrm{E}_{\boldsymbol{H}}[\boldsymbol{H}\boldsymbol{x}\boldsymbol{x}^{\mathrm{H}}\boldsymbol{H}^{\mathrm{H}}]$ do not contribute to the mutual information in the hard decision system. This is because , with symmetric two-level quantization, the amplitude of the received signal does not contribute to the mutual information. That means that the channel coefficients have to be correlated, otherwise $\mathrm{E}_{\boldsymbol{H}}[\boldsymbol{H}\boldsymbol{x}\boldsymbol{x}^{\mathrm{H}}\boldsymbol{H}^{\mathrm{H}}]$ is diagonal and the mutual information is zero up to the second order. Nevertheless, in most systems of practical interest, the correlation between the channel coefficients, whether temporal or spatial, exists even in multipath rich mobile environments, thus $\mathrm{E}_{\boldsymbol{H}}[\boldsymbol{H}\boldsymbol{x}\boldsymbol{x}^{\mathrm{H}}\boldsymbol{H}^{\mathrm{H}}]$ is a rather dense matrix whose Frobenius norm is dominated by the off-diagonal elements rather than the diagonal entries. Thus the low-SNR penalty due to the hard-decision is nearly 1.96 dB for almost all practical channels. This confirms that low-resolution sampling in the low-SNR regime performs adequately regardless of the channel model and the kind of CSI available at the receiver while reducing power consumption.

2) Proof of Theorem 6: We start again with the definition of mutual information

$$\begin{aligned} I(\boldsymbol{x};\boldsymbol{r}) &= H(\boldsymbol{r}) - H(\boldsymbol{r}|\boldsymbol{x}) \\ &= H(\mathrm{sign}(\boldsymbol{H}\boldsymbol{x}+\boldsymbol{\eta})) - H(\mathrm{sign}(\boldsymbol{H}\boldsymbol{x}+\boldsymbol{\eta})|\boldsymbol{x}), \end{aligned} \quad (51)$$

then we use, Corollary 1 and Corollary 2 with $\varepsilon = \frac{1}{\sigma_\eta}$ and $g(\boldsymbol{x}) = \boldsymbol{H}\boldsymbol{x}$ to get the following asymptotic expression:

$$\begin{aligned} &I(\boldsymbol{x};\boldsymbol{r}) \\ &= 2N\ln 2 - \frac{2}{\pi}\frac{1}{\sigma_\eta^2}\|\mathrm{E}_{\boldsymbol{x},\boldsymbol{H}}[\boldsymbol{H}\boldsymbol{x}]\|_2^2 \\ &\quad - \frac{1}{\sigma_\eta^4}\left(\frac{2}{\pi^2}\mathrm{tr}\left(\left(\mathrm{nondiag}(\mathrm{E}_{\boldsymbol{x},\boldsymbol{H}}[\boldsymbol{H}\boldsymbol{x}\boldsymbol{x}^{\mathrm{H}}\boldsymbol{H}^{\mathrm{H}}])\right)^2\right)\right. \\ &\quad - \frac{4}{3\pi}\|\mathrm{E}_{\boldsymbol{x},\boldsymbol{H}}[\boldsymbol{H}\boldsymbol{x}] \circ \mathrm{E}_{\boldsymbol{x},\boldsymbol{H}}[\boldsymbol{H}\boldsymbol{x}\circ\boldsymbol{H}\boldsymbol{x}\circ\boldsymbol{H}\boldsymbol{x}]\|_1^1 \\ &\quad \left.+ \frac{4}{3\pi^2}\|\mathrm{E}_{\boldsymbol{x},\boldsymbol{H}}[\boldsymbol{H}\boldsymbol{x}]\|_4^4\right) - 2\,N\ln 2 + \frac{2}{\pi}\frac{1}{\sigma_\eta^2}\mathrm{E}_{\boldsymbol{x}}[\|\mathrm{E}_{\boldsymbol{H}}[\boldsymbol{H}\boldsymbol{x}]\|_2^2] \\ &\quad + \frac{1}{\sigma_\eta^4}\mathrm{E}_{\boldsymbol{x}}\left[\frac{2}{\pi^2}\mathrm{tr}\left(\left(\mathrm{nondiag}(\mathrm{E}_{\boldsymbol{H}}[\boldsymbol{H}\boldsymbol{x}\boldsymbol{x}^{\mathrm{H}}\boldsymbol{H}^{\mathrm{H}}])\right)^2\right)\right. \\ &\quad - \frac{4}{3\pi}\|\mathrm{E}_{\boldsymbol{H}}[\boldsymbol{H}\boldsymbol{x}] \circ \mathrm{E}_{\boldsymbol{H}}[\boldsymbol{H}\boldsymbol{x}\circ\boldsymbol{H}\boldsymbol{x}\circ\boldsymbol{H}\boldsymbol{x}]\|_1^1 \\ &\quad \left.+ \frac{4}{3\pi^2}\|\mathrm{E}_{\boldsymbol{H}}[\boldsymbol{H}\boldsymbol{x}]\|_4^4\right] + o(\frac{1}{\sigma_\eta^4}) \\ &= \frac{2}{\sigma_\eta^4\pi^2}\mathrm{tr}\left(\mathrm{E}_{\boldsymbol{x}}[\left(\mathrm{nondiag}(\mathrm{E}_{\boldsymbol{H}}[\boldsymbol{H}\boldsymbol{x}\boldsymbol{x}^{\mathrm{H}}\boldsymbol{H}^{\mathrm{H}}])\right)^2]\right. \\ &\quad \left. - \left(\mathrm{nondiag}(\mathrm{E}_{\boldsymbol{x},\boldsymbol{H}}[\boldsymbol{H}\boldsymbol{x}\boldsymbol{x}^{\mathrm{H}}\boldsymbol{H}^{\mathrm{H}}])\right)^2\right) + o(\frac{1}{\sigma_\eta^4}), \end{aligned}$$

where the last step follows from the fact that the channel matrix $\boldsymbol{H}$ has zero-mean. We note that since $\boldsymbol{H}$ has a proper distribution, then $g(\boldsymbol{x}) = \boldsymbol{H}\boldsymbol{x}$ also has a zero-mean proper distribution, fulfilling $p(\boldsymbol{H}) = p(\mathrm{j}\boldsymbol{H}\boldsymbol{x})$. This yields the result stated by the theorem and completes the proof. Note that the condition $\mathrm{E}_{\boldsymbol{x},\boldsymbol{H}}[\|\boldsymbol{H}(\boldsymbol{x})\|_4^{4+\varepsilon}] < \delta$ for some finite constants $\varepsilon, \delta > 0$ ensures that the remainder of the expansion is asymptotically negligible as shown in the coherent case (see Section IV-A).

C. IID Block Rayleigh Fading MIMO Channels

We consider as an example a point-to-point quantized MIMO channel where the transmitter employs M' antennas and the receiver has N' antennas. We assume a block-Rayleigh fading model [60], in which the channel propagation matrix $\boldsymbol{H}' \in \mathbb{C}^{M' \times N'}$ remains constant for a coherence interval

Authorized licensed use limited to: Access paid by The UC Irvine Libraries. Downloaded on May 08,2021 at 22:45:13 UTC from IEEE Xplore. Restrictions apply.

of length T symbols, and then changes to a new independent value. The entries of the channel matrix are i.i.d. zero-mean complex circular Gaussian with unit variance. The channel realizations are unknown to both the transmitter and receiver. At each coherence interval, a sequence of vectors $x_1, \dots, x_T$ are transmitted at each time slot via the multiple antennas. The transmitted and received signal matrices are then related as follows (total dimensions: $N = TN'$ and $M = TM'$)

$$\underbrace{\begin{bmatrix} \boldsymbol{y}_1 \\ \boldsymbol{y}_2 \\ \vdots \\ \boldsymbol{y}_T \end{bmatrix}}_{\boldsymbol{y}} = \underbrace{\begin{bmatrix} \boldsymbol{H}' & 0 & \cdots & 0 \\ 0 & \boldsymbol{H}' & \cdots & 0 \\ 0 & 0 & \ddots & 0 \\ 0 & 0 & \cdots & \boldsymbol{H}' \end{bmatrix}}_{\boldsymbol{H}} \cdot \underbrace{\begin{bmatrix} \boldsymbol{x}_1 \\ \boldsymbol{x}_2 \\ \vdots \\ \boldsymbol{x}_T \end{bmatrix}}_{\boldsymbol{x}} + \underbrace{\begin{bmatrix} \boldsymbol{\eta}_1 \\ \boldsymbol{\eta}_2 \\ \vdots \\ \boldsymbol{\eta}_T \end{bmatrix}}_{\boldsymbol{\eta}}. \tag{52}$$

Then the expected value of the received signal conditioned on the input is given by

$$\mathrm{E}[\boldsymbol{H}\boldsymbol{x}\boldsymbol{x}^{\mathrm{H}}\boldsymbol{H}^{\mathrm{H}}|\boldsymbol{x}] = \begin{bmatrix} \mathrm{E}[\boldsymbol{H}'\boldsymbol{x}_1\boldsymbol{x}_1^{\mathrm{H}}\boldsymbol{H}'^{\mathrm{H}}] & \cdots & \mathrm{E}[\boldsymbol{H}'\boldsymbol{x}_1\boldsymbol{x}_T^{\mathrm{H}}\boldsymbol{H}'^{\mathrm{H}}] \\ \mathrm{E}[\boldsymbol{H}'\boldsymbol{x}_2\boldsymbol{x}_1^{\mathrm{H}}\boldsymbol{H}'^{\mathrm{H}}] & \cdots & \mathrm{E}[\boldsymbol{H}'\boldsymbol{x}_2\boldsymbol{x}_T^{\mathrm{H}}\boldsymbol{H}'^{\mathrm{H}}] \\ \ddots & \ddots & \ddots \\ \mathrm{E}[\boldsymbol{H}'\boldsymbol{x}_T\boldsymbol{x}_1^{\mathrm{H}}\boldsymbol{H}'^{\mathrm{H}}] & \cdots & \mathrm{E}[\boldsymbol{H}'\boldsymbol{x}_T\boldsymbol{x}_T^{\mathrm{H}}\boldsymbol{H}'^{\mathrm{H}}] \end{bmatrix}. \tag{53}$$

Since $\boldsymbol{H}'$ is i.i.d. distributed, it can be shown that $\mathrm{E}_{\boldsymbol{H}'}[\boldsymbol{H}'\boldsymbol{x}_i\boldsymbol{x}_j^{\mathrm{H}}\boldsymbol{H}'^{\mathrm{H}}] = \boldsymbol{x}_i^{\mathrm{T}}\boldsymbol{x}_j^* \cdot \mathbf{I}_{N'}$. Therefore, we have

$$\mathrm{E}[\boldsymbol{H}\boldsymbol{x}\boldsymbol{x}^{\mathrm{H}}\boldsymbol{H}^{\mathrm{H}}|\boldsymbol{x}] = (\boldsymbol{X}\cdot\boldsymbol{X}^{\mathrm{H}}) \otimes \mathbf{I}_{N'}, \tag{54}$$

where the rows of the matrix $\boldsymbol{X} \in \mathbb{C}^{T\times M'}$ are the vectors $\boldsymbol{x}_i^{\mathrm{T}}$, for $1 \le i \le T$. With this, (49) asymptotically becomes

$$I(\boldsymbol{x};\boldsymbol{r}) = \frac{N'}{2}\left(\frac{2}{\pi}\frac{1}{\sigma_\eta^2}\right)^2 \mathrm{tr}\left\{\mathrm{E}\left[(\mathrm{nondiag}(\boldsymbol{X}\cdot\boldsymbol{X}^{\mathrm{H}}))^2\right] - (\mathrm{nondiag}(\mathrm{E}[\boldsymbol{X}\cdot\boldsymbol{X}^{\mathrm{H}}]))^2\right\} + o(\frac{1}{\sigma_\eta^4}), \tag{55}$$

in nats per coherence interval, while for the ideal case, we get from (50) (see also [52])

$$I(\boldsymbol{x};\boldsymbol{y}) = \frac{N'}{2}\left(\frac{1}{\sigma_\eta^2}\right)^2 \mathrm{tr}\left\{\mathrm{E}\left[(\boldsymbol{X}\cdot\boldsymbol{X}^{\mathrm{H}})^2\right] - (\mathrm{E}[\boldsymbol{X}\cdot\boldsymbol{X}^{\mathrm{H}}])^2\right\} + o(\frac{1}{\sigma_\eta^4}). \tag{56}$$

Now, assuming i.i.d. Gaussian inputs with $\mathrm{E}[\boldsymbol{X}\boldsymbol{X}^{\mathrm{H}}] = P_{\mathrm{Tr}} \cdot \mathbf{I}_T$, then we obtain finally (c.f. expectation (21))

$$I(\boldsymbol{x};\boldsymbol{r}) = \frac{N'}{2}\left(\frac{2}{\pi}\frac{P_{\mathrm{Tr}}}{\sigma_\eta^2}\right)^2 T(T-1) + o(\frac{1}{\sigma_\eta^4})$$
$$I(\boldsymbol{x};\boldsymbol{y}) = \frac{N'}{2}\left(\frac{P_{\mathrm{Tr}}}{\sigma_\eta^2}\right)^2 T^2 + o(\frac{1}{\sigma_\eta^4}). \tag{57}$$

Evidently, in order for $I(\boldsymbol{x};\boldsymbol{r})$ and $I(\boldsymbol{x};\boldsymbol{y})$ to be equal with the same power, we need to increase the number of one-bit receive antennas N' by roughly a factor of $\pi^2/4$ when the coherence interval satisfies $T \gg 1$. The same result has been obtained in [44], [45] with a pilot-based scheme and using the Bussgang decomposition of the nonlinear quantizer.

D. SIMO Channels With Delay Spread and Receive Correlation at Low SNR

As a further example, we use the result from Theorem 6 to compute the low SNR mutual information of a frequency-selective single input multi-output (SIMO) channel with delay spread and receive correlation both in time and space and obtain the asymptotic achievable rate under average and peak power constraints. The quantized output of the considered model at time k is

$$\boldsymbol{r}_k = Q(\boldsymbol{y}_k)$$
$$\boldsymbol{y}_k = \sum_{t=0}^{T-1} \boldsymbol{h}_k[t]x_{k-t} + \boldsymbol{\eta}_k \in \mathbb{C}^{N'}, \tag{58}$$

where the noise process $\{\boldsymbol{\eta}_k\}$ is i.i.d. in time and space, while the T fading processes $\{\boldsymbol{h}_k[t]\}$ at each tap t are assumed to be independent zero-mean proper complex Gaussian processes. Furthermore, we assume a separable temporal spatial correlation model, i.e.

$$\mathrm{E}[\boldsymbol{h}_k[t]\boldsymbol{h}_{k'}[t']^{\mathrm{H}}] = \boldsymbol{C}_h \cdot c_h(k-k')\alpha_t\delta[t-t']. \tag{59}$$

Here, $\boldsymbol{C}_h$ denotes the receive correlation matrix, $c_h(k)$ is the autocorrelation function of the fading process, and the scalars α_i represent the power-delay profile. The correlation parameters can be normalized so that

$$\mathrm{tr}(\boldsymbol{C}_h) = N',\ c_h(0) = 1 \text{ and } \sum_{t=0}^{T-1}\alpha_t = 1. \tag{60}$$

In other words, the energy in each receive antenna's impulse response equals one on average. On the other hand we assume that the transmit signal x_k is subject to an average power constraint $\mathrm{E}[|x_k|^2] \le P_{\mathrm{Tr}}$ and a peak power constraint $|x_k|^2 \le \beta \cdot P_{\mathrm{Tr}}$, $\forall k$, with $\beta \ge 1$. It should be pointed out that a peak power constraint constitutes a stronger condition than necessary for the validity of Theorem 6, involving just a fourth-order moment constraint on the input. We consider now a time interval of length n (a block of n transmissions). Collect a vector sequence $\boldsymbol{y}_k$ of length n into the vector $\boldsymbol{y}$ as

$$\boldsymbol{y}^{(n)} = \left[\boldsymbol{y}_{n-1}^{\mathrm{T}}, \dots, \boldsymbol{y}_0^{\mathrm{T}}\right]^{\mathrm{T}}, \tag{61}$$

and form the block cyclic-shifted matrix $\boldsymbol{H}^{(n)} \in \mathbb{C}^{(N'n)\times n}$

$$\boldsymbol{H}^{(n)} = \begin{bmatrix} \boldsymbol{h}_{n-1}[0] & \cdots & \boldsymbol{h}_{n-1}[T-1] & 0 & \cdots \\ & \ddots & & & \ddots \\ \ddots & & & \ddots & \\ \cdots & \boldsymbol{h}_0[T-1] & 0 & \cdots & 0 \quad \boldsymbol{h}_0[0] \end{bmatrix}. \tag{62}$$

With

$$\boldsymbol{x}^{(n)} = [x_{n-1}, \dots, x_0]^{\mathrm{T}}, \tag{63}$$

and $\boldsymbol{\eta}^{(n)}$ and $\boldsymbol{r}^{(n)}$ defined similar to $\boldsymbol{y}^{(n)}$, the following quantized space-time model may be formulated as a (loose) approximation of (58), where the resulting dimensions are $N = N'n$ and $M = n$

$$\boldsymbol{r}^{(n)} = Q(\boldsymbol{y}^{(n)}) = Q\left(\boldsymbol{H}^{(n)}\boldsymbol{x}^{(n)} + \boldsymbol{\eta}^{(n)}\right). \tag{64}$$

Authorized licensed use limited to: Access paid by The UC Irvine Libraries. Downloaded on May 08,2021 at 22:45:13 UTC from IEEE Xplore. Restrictions apply.

1) Asymptotic Achievable Rate: Now, we elaborate on the asymptotic information rate of this channel setting.

Proposition 1: If $c_h(k)$ is square-summable, then the mutual information of the described space-time model admits the following asymptotic maximum rate, under an average power constraint $\mathrm{E}[|x_k|^2] \leq P_{\mathrm{Tr}}$ and a peak power constraint $|x_k|^2 \leq \beta \cdot P_{\mathrm{Tr}}, \forall k$, with $\beta \geq 1$

$$\lim_{n\to\infty} \max_{\substack{p(\boldsymbol{x}^{(n)})\\ \text{s.t. power constraints}}} \frac{1}{n} I(\boldsymbol{x}^{(n)};\boldsymbol{r}^{(n)}) = \left(\frac{2}{\pi}\frac{P_{\mathrm{Tr}}}{\sigma_\eta^2}\right)^2 U(\beta) + o(\frac{1}{\sigma_\eta^4}), \tag{65}$$

where

$$U(\beta) = \begin{cases} \beta\cdot\zeta + (\beta-1)\chi & \text{for } \beta(\zeta+\chi) \geq 2\chi \\ \beta^2\frac{(\zeta+\chi)^2}{4\chi} & \text{else,} \end{cases} \tag{66}$$

$$\zeta = \mathrm{tr}(\boldsymbol{C}_h^2)\sum_{k=1}^{\infty} c_h(k)^2 \tag{67}$$

and

$$\chi = \frac{1}{2}\mathrm{tr}((\mathrm{nondiag}(\boldsymbol{C}_h))^2)c_h(0). \tag{68}$$

Proof: First, we establish the stated result as an upper bound on the asymptotic rate for any distribution fulfilling the average and peak power constraints, and then we show that it can actually be achieved with an appropriate transmission strategy. Due to the peak power constraints, the conditions of Theorem 6 are satisfied; thus the second order approximation (49) is valid. A tight upper bound is obtained by looking at the maximal value that can be achieved by the expression (49) up to second order. We do this in two steps. We first maximize the trace expression in (49) under a prescribed average power per symbol γ. The maximum can be, in turn, upper bounded by the supremum of the first term minus the infimum of the second term under the prescribed average power and the original peak power constraint. After that, we perform an optimization over the parameter γ itself. That is

$$\begin{aligned} I(\boldsymbol{x}^{(n)};\boldsymbol{r}^{(n)}) \leq \frac{1}{2}\left(\frac{2}{\pi}\frac{1}{\sigma_\eta^2}\right)^2 \max_{0\leq\gamma\leq 1} \Bigg\{ & \\ \sup_{\substack{|x_k|^2\leq\beta P_{\mathrm{Tr}},\forall k\\ \mathrm{E}[\|\boldsymbol{x}^{(n)}\|^2]=\gamma P_{\mathrm{Tr}}\cdot n}} \mathrm{tr}\left(\mathrm{E}\left[(\mathrm{nondiag}(\mathrm{E}[\boldsymbol{H}^{(n)}\boldsymbol{x}^{(n)}\boldsymbol{x}^{(n),\mathrm{H}}\boldsymbol{H}^{(n),\mathrm{H}}|\boldsymbol{x}]))^2\right]\right) & \\ - \inf_{\substack{|x_k|^2\leq\beta P_{\mathrm{Tr}},\forall k\\ \mathrm{E}[\|\boldsymbol{x}^{(n)}\|^2]=\gamma P_{\mathrm{Tr}}\cdot n}} \mathrm{tr}\left((\mathrm{nondiag}(\mathrm{E}[\boldsymbol{H}^{(n)}\mathrm{E}[\boldsymbol{x}^{(n)}\boldsymbol{x}^{(n),\mathrm{H}}]\boldsymbol{H}^{(n),\mathrm{H}}]))^2\right)\Bigg\} & \\ + o(\frac{1}{\sigma_\eta^4}). & \end{aligned} \tag{69}$$

Evaluating the expectation with respect to the channel realizations, we get

$$\mathrm{E}[\boldsymbol{H}^{(n)}\boldsymbol{x}^{(n)}\boldsymbol{x}^{(n),\mathrm{H}}\boldsymbol{H}^{(n),\mathrm{H}}] = \boldsymbol{D}\otimes\boldsymbol{C}_h, \tag{70}$$

with

$$d_{k,k'} = c_h(k-k')\sum_{t=0}^{T-1}\alpha_t x_{k-t}x_{k'-t}^* \text{ for } k,k'\in\{0,\ldots,n-1\}. \tag{71}$$

Therefore

$$\begin{aligned} &\mathrm{tr}\left((\mathrm{nondiag}(\mathrm{E}[\boldsymbol{H}^{(n)}\boldsymbol{x}^{(n)}\boldsymbol{x}^{(n),\mathrm{H}}\boldsymbol{H}^{(n),\mathrm{H}}|\boldsymbol{x}]))^2\right) \\ &= \sum_{k=0}^{n-1}\sum_{\substack{k'=0\\ k'\neq k}}^{n-1}\mathrm{tr}(\boldsymbol{C}_h^2)c_h(k-k')^2\left|\sum_{t=0}^{T-1}\alpha_t x_{k-t}x_{k'-t}^*\right|^2 \\ &\quad + \sum_{k=0}^{n-1}\mathrm{tr}((\mathrm{nondiag}(\boldsymbol{C}_h))^2)c_h(0)^2\left|\sum_{t=0}^{T-1}\alpha_t|x_{k-t}|^2\right|^2. \end{aligned} \tag{72}$$

Using the Minkowski and Cauchy-Schwarz expectation inequalities, i.e., $\mathrm{E}[|z_1+z_2|^2]^{\frac{1}{2}} \leq \mathrm{E}[|z_1|^2]^{\frac{1}{2}} + \mathrm{E}[|z_2|^2]^{\frac{1}{2}}$, and $\mathrm{E}[|z_1z_2|] \leq \mathrm{E}[|z_1|^2]^{\frac{1}{2}}\mathrm{E}[|z_2|^2]^{\frac{1}{2}}$, respectively, we have

$$\mathrm{E}\left[\left|\sum_{t=0}^{T-1}\alpha_t|x_{k-t}|^2\right|^2\right] \leq \left(\sum_{t=0}^{T-1}\alpha_t\mathrm{E}\left[|x_{k-t}|^4\right]^{\frac{1}{2}}\right)^2, \tag{73}$$

and

$$\begin{aligned} \mathrm{E}\left[\left|\sum_{t=0}^{T-1}\alpha_t x_{k-t}x_{k'-t}^*\right|^2\right] &\leq \left(\sum_{t=0}^{T-1}\alpha_t\left(\mathrm{E}\left[|x_{k-t}x_{k'-t}^*|^2\right]\right)^{\frac{1}{2}}\right)^2 \\ &\leq \left(\sum_{t=0}^{T-1}\alpha_t\mathrm{E}\left[|x_{k-t}|^4\right]^{\frac{1}{4}}\mathrm{E}\left[|x_{k'-t}|^4\right]^{\frac{1}{4}}\right)^2, \end{aligned} \tag{74}$$

with equality if the variables are equal. In addition, $\mathrm{E}\left[|x_k|^4\right]$ is a linear functional in terms of $p(x_k)$ and achieves its maximum under average and peak power constraints at an extremal distribution [61], i.e., a two-mass distribution at zero and peak power. Therefore, the supremum of the first trace term is achieved when all x_k inputs take, simultaneously during the considered time interval, either the value zero, or the peak value β with a duty cycle of $\gamma\beta^{-1}$. On the other hand, the infimum of the second trace expression is obtained, under the prescribed average power, when $\mathrm{E}[\boldsymbol{x}\boldsymbol{x}^{\mathrm{H}}] = \gamma P_{\mathrm{Tr}}\mathbf{I}_n$. Calculation shows that

$$\begin{aligned} &\frac{1}{n}I(\boldsymbol{x}^{(n)};\boldsymbol{r}^{(n)}) \\ &\leq \max_{0\leq\gamma\leq1}\left(\frac{2}{\pi}\frac{P_{\mathrm{Tr}}}{\sigma_\eta^2}\right)^2\left(\sum_{t=0}^{T-1}\alpha_t\right)^2\Bigg[\gamma\beta\cdot\underbrace{\mathrm{tr}(\boldsymbol{C}_h^2)\sum_{k=1}^{n-1}(1-\frac{k}{n})c_h(k)^2}_{\zeta^{(n)}} \\ &\quad + \gamma(\beta-\gamma)\underbrace{\frac{1}{2}\mathrm{tr}((\mathrm{nondiag}(\boldsymbol{C}_h))^2)c_h(0)^2}_{\chi}\Bigg] + o(\frac{1}{\sigma_\eta^4}). \end{aligned} \tag{75}$$

Now, the maximization over γ delivers

$$\gamma_{\mathrm{opt}} = \min\{1, \beta\frac{\zeta^{(n)}+\chi}{2\chi}\}. \tag{76}$$

Authorized licensed use limited to: Access paid by The UC Irvine Libraries. Downloaded on May 08,2021 at 22:45:13 UTC from IEEE Xplore. Restrictions apply.

Thus, taking the limit $n \to \infty$ yields $\zeta^{(n)} \to \zeta$ as in (67) and by the normalizations in (60), we end up with the result of the proposition as an upper bound.[4]

We next turn to the question of how to achieve the maximum rate stated by Proposition 1 is achievable. A closer examination of (69) demonstrates that the maximum rate could be achieved if the input distribution satisfies the following condition, for any time instants k and l within the block of length n:

$$x_k x_l^* = a e^{j\Omega(k-l)}, \quad (77)$$

for some $\Omega \neq 0$ and random $a \in \{0, \sqrt{\beta \cdot P_{\mathrm{Tr}}}\}$, while having $\mathrm{E}[\boldsymbol{x}^{(n)}\boldsymbol{x}^{(n),\mathrm{H}}] = \gamma P_{\mathrm{Tr}} \mathbf{I}_n$ as already mentioned in the proof of Proposition 1. Clearly an *on-off frequency-shift keying* (OOFSK) modulation for the input, as follows, can fulfill these conditions

$$x_k = Z \cdot e^{jk\Omega}, \quad k \in \{1, \ldots, n\}, \quad (78)$$

where Z takes the value $\sqrt{\beta P_{\mathrm{Tr}}}$ with probability $\gamma_{\mathrm{opt}}\beta^{-1}$ and zero with probability $(1 - \gamma_{\mathrm{opt}}\beta^{-1})$, and Ω is uniformly distributed over the set $\{\frac{2\pi}{n}, \ldots, \frac{2\pi(n-1)}{n}\}$. This is similar to the results of the unquantized case [54], [62]. □

2) Discussion: We notice from (76) that the average power constraint $\mathrm{E}[|x_k|^2] \leq P_{\mathrm{Tr}}$ is only active when $\beta(\zeta + \chi) \geq 1$, which means that it is not necessarily optimal to utilize the total available or allowed average power especially if a tight peak power constraint is present. In addition, if we impose only a peak power constraint, i.e. $\beta = 1$, then if $\zeta < \chi$ the on-off strategy with the zero symbol ($a = 0$) is required to approach the capacity. We observe also from Proposition 1 that spreading the power over different taps does not affect the low SNR rate, while receiver correlation is beneficial due to two effects. First the mutual information increases with χ defined in (68) which is related to the norm of the off-diagonal elements of $\boldsymbol{C}_h$. Second, under the normalization $\mathrm{tr}(\boldsymbol{C}_h) = N'$, the Frobenius norm $\mathrm{tr}(\boldsymbol{C}_h^2)$ increases with more correlation among the receive antennas, and consequently, higher rates at low SNR can be achieved due to relation (67). In fact, both spatial and temporal correlations are extremely beneficial at low SNR, even more than in the unquantized case. Besides we note that the achievability of the rate stated in Proposition 1, as discussed previously, is obtained at the cost of burstiness in frequency which may not compatible with the specifications imposed on some systems.[5] Therefore, it is interesting to look at the asymptotic rate of i.i.d. input symbols drawn from the set $\{-\sqrt{\beta P_{\mathrm{Tr}}}, 0, \sqrt{\beta P_{\mathrm{Tr}}}\}$. In that case it turns out by (49) that

$$\lim_{n\to\infty} \frac{1}{n} I_{\mathrm{IID}}(\boldsymbol{x}^{(n)}; \boldsymbol{r}^{(n)}) = \max_{0\leq\gamma\leq 1} \left(\frac{2}{\pi}\frac{P_{\mathrm{Tr}}}{\sigma_\eta^2}\right)^2 \Bigg[\gamma^2 \zeta^{(n)} \sum_{t=0}^{T-1} \alpha_t^2 + \gamma(\beta - \gamma)\chi \left(\sum_{t=0}^{T-1} \alpha_t\right)^2\Bigg] + o(1/\sigma_\eta^4). \quad (79)$$

Here, we observe that, contrary to the FSK-like scheme, the mutual information with i.i.d input is negatively affected by the delay spread since $\sum_{t=0}^{T-1} \alpha_t^2 \leq 1$ by the normalization (60). Nevertheless for the case $\chi \gg \zeta$, i.e. low temporal correlation (high Doppler spread), the gap to the maximum rate in Proposition 1 vanishes, as demonstrated in Fig. 9.

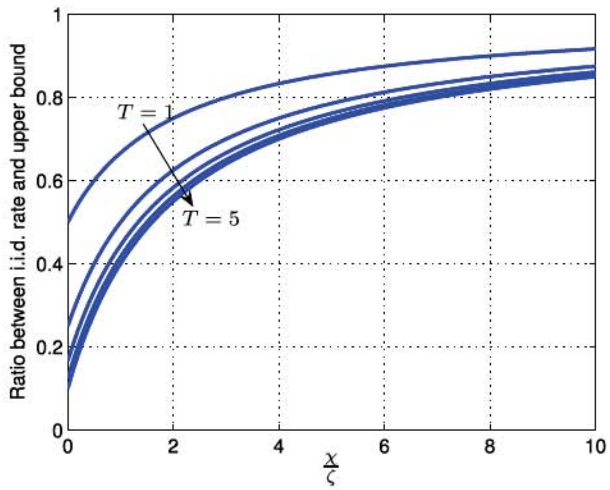

Fig. 9. Ratio of i.i.d. rate (79) and maximum rate (65) vs. the spatial-to-temporal coherence ratio $\frac{\chi}{\zeta}$ for $\beta = 2$ and uniform delay spread, i.e. $\alpha_t = \frac{1}{T}$.

VI. Conclusion

Motivated by the simplicity of one-bit ADCs for sampling large dimensional signals, we provided a general second-order asymptotic analysis for the entropy of one-bit quantized vector signals. We used these results to evaluate the mutual information around zero SNR for a wide class of channel models. We have shown that the reduction of low SNR channel capacity by a factor of $2/\pi$ due to 1-bit quantization holds for the general MIMO case with uncorrelated noise. We also showed that QPSK is uniquely optimal at low SNR, in contrast to the ideal case with infinite resolution, where any proper zero-mean distribution is asymptotically optimal. In massive MIMO, the capacity loss can be compensated, up the second order in SNR by increasing the number of receiving antennas by a factor of $\pi/2$.

Furthermore, the non-coherent MIMO channel was studied in detail. First, closed-form expressions were derived for the non-coherent block-Rayleigh fading SISO with QPSK signals. Then, it was shown that the $2/\pi$ low-SNR loss due to 1-bit quantization still holds for all channels of practical interest. Finally, the asymptotic performance of SIMO Channels with delay spread and receive correlation was considered at low SNR under peak and average power constraints, where OOFSK modulation is shown to be optimal.

Appendix A
Proof of Theorem 1

We aim at the derivation of the second order approximation (Taylor expansion) of the entropy $H(\boldsymbol{r})$, where $\boldsymbol{r} = \mathrm{sign}(\boldsymbol{y}) = \mathrm{sign}(\varepsilon \boldsymbol{x} + \boldsymbol{\eta})$, with respect to ε. Thereby, we assume that the vector $\boldsymbol{\eta}$ is i.i.d. Gaussian distributed with unit variance and $\boldsymbol{x}$ has a general distribution. As will be shown in the

[4]Observe that ζ and χ are indicators for the temporal and spatial coherence, respectively.

[5]Note that such observations hold also in the unquantized case [54].

Authorized licensed use limited to: Access paid by The UC Irvine Libraries. Downloaded on May 08,2021 at 22:45:13 UTC from IEEE Xplore. Restrictions apply.

following, this second order Taylor expansion is a function of the moments of the distribution of x, which have to fulfill certain conditions. For simplicity, we consider first the real-valued case for the computation of the second order approximation of the entropy $H(\mathrm{sign}(\varepsilon \boldsymbol{x}+\boldsymbol{\eta}))$ assuming that $\boldsymbol{x}$ has a real-valued distribution and $\boldsymbol{\eta}$ follows a real-valued Gaussian distribution with variance $\frac{1}{2}$. The generalization to the complex case can be obtained based on the real-valued representation of the complex channel and is performed at the end of the proof. The probability mass function $P_\epsilon(\boldsymbol{r})$ of the random vector $\boldsymbol{r}=\mathrm{sign}(\varepsilon \boldsymbol{x}+\boldsymbol{\eta}) \in \{\pm 1\}^N$ is given by

$$P_\epsilon(\boldsymbol{r}) = P(\boldsymbol{r}\circ\boldsymbol{y} \in \mathbb{R}_+^N) = \mathrm{E}_{\boldsymbol{x}} \int_{\mathbb{R}_+^N} p_\epsilon(\boldsymbol{r}\circ\boldsymbol{y}|\boldsymbol{x})\mathrm{d}\boldsymbol{y}, \quad (80)$$

where

$$p_\epsilon(\boldsymbol{y}|\boldsymbol{x}) = \frac{1}{\pi^{N/2}}\mathrm{e}^{-\|\boldsymbol{y}-\varepsilon\boldsymbol{x}\|_2^2}. \quad (81)$$

We also have the general expression of the entropy (in nats) of random vector $\boldsymbol{r}$ as

$$H(\boldsymbol{r}) = \sum_{\boldsymbol{r}\in\{\pm 1\}^N} -P_\varepsilon(\boldsymbol{r})\ln P_\varepsilon(\boldsymbol{r}). \quad (82)$$

Next, based on the derivatives of the function $-z\ln z$, we calculate the second order expansion of the entropy with respect to ε. For that, we first notice that the linear and cubic terms of the Taylor expansion vanish due to the fact that the entropy function $H(\mathrm{sign}(\varepsilon \boldsymbol{x}+\boldsymbol{\eta}))$ is an even function with respect to ε since $H(\mathrm{sign}(\varepsilon \boldsymbol{x}+\boldsymbol{\eta})) = H(\mathrm{sign}(-\varepsilon \boldsymbol{x}+\boldsymbol{\eta}))$. Additionally, since $P_\varepsilon(\boldsymbol{r})$ is a probability mass function, i.e., $\sum_{\boldsymbol{r}} P_\varepsilon(\boldsymbol{r})=1$, we have

$$\sum_{\boldsymbol{r}} P_\varepsilon^{(k)}(\boldsymbol{r}) = 0, \quad (83)$$

for any k-th derivative of $P_\varepsilon^{(k)}(\boldsymbol{r})$ with respect to ε. Based on these observations, we get the following second order expansion

$$H(\boldsymbol{r}) = \sum_{\boldsymbol{r}} -P_0(\boldsymbol{r})\ln P_0(\boldsymbol{r}) - \varepsilon^2\frac{P_0'(\boldsymbol{r})^2}{2P_0(\boldsymbol{r})} - \varepsilon^4\left(\frac{P_0'(\boldsymbol{r})^4}{12P_0(\boldsymbol{r})^3} - \frac{P_0'(\boldsymbol{r})^2P_0''(\boldsymbol{r})}{4P_0(\boldsymbol{r})^2} + \frac{P_0''(\boldsymbol{r})^2}{8P_0(\boldsymbol{r})} + \frac{P_0'(\boldsymbol{r})P_0^{(3)}(\boldsymbol{r})}{6P_0(\boldsymbol{r})}\right) + \Delta H(\boldsymbol{r}), \quad (84)$$

where

$$P_0(\boldsymbol{r}) = \int_{\mathbb{R}_+^N} \frac{2}{\pi^{\frac{N}{2}}}\mathrm{e}^{-\|\boldsymbol{y}\|_2^2}\mathrm{d}\boldsymbol{y} = \frac{1}{2^N}, \quad (85)$$

and $P_0'(\boldsymbol{r})$, $P_0''(\boldsymbol{r})$ and $P_0'(\boldsymbol{r})P_0^{(3)}(\boldsymbol{r})$ are the first, second and third order derivatives of $P_\varepsilon(\boldsymbol{r})$ at $\varepsilon=0$, which will be derived in the following. To this end, we utilize the following derivatives of the unquantized output distribution $p_\epsilon(\boldsymbol{y}|\boldsymbol{x}) = \frac{1}{\pi^{N/2}}\mathrm{e}^{-\|\boldsymbol{y}-\varepsilon\boldsymbol{x}\|_2^2}$

$$p_0'(\boldsymbol{y}|\boldsymbol{x}) = \frac{1}{\pi^{N/2}}\mathrm{e}^{-\|\boldsymbol{y}\|_2^2}2\boldsymbol{y}^{\mathrm{T}}\boldsymbol{x}, \quad (86)$$

$$p_0''(\boldsymbol{y}|\boldsymbol{x}) = \frac{2}{\pi^{N/2}}\mathrm{e}^{-\|\boldsymbol{y}\|_2^2}(2(\boldsymbol{y}^{\mathrm{T}}\boldsymbol{x})^2 - \|\boldsymbol{x}\|_2^2), \quad (87)$$

$$p_0^{(3)}(\boldsymbol{y}|\boldsymbol{x}) = \frac{6}{\pi^{N/2}}\mathrm{e}^{-\|\boldsymbol{y}\|_2^2}2\boldsymbol{y}^{\mathrm{T}}\boldsymbol{x}(\frac{2}{3}(\boldsymbol{y}^{\mathrm{T}}\boldsymbol{x})^2 - \|\boldsymbol{x}\|_2^2). \quad (88)$$

Further, we express $P_\varepsilon^{(k)}(\boldsymbol{r})$ in terms of $p_\varepsilon^{(k)}(\boldsymbol{y})$, i.e., by interchanging the derivative of (80) with respect to ε with the integral operators. For that to hold, let us assume that $p_\varepsilon^{(k)}(\boldsymbol{y})$ is decaying sufficiently fast and thus integrable on $\mathbb{R}_+^N$ (a condition for the expansion (84) to hold with asymptotically vanishing remainder term is discussed at the end of the appendix)[6]. Then, by the dominated convergence theorem, we evaluate the first order derivative as

$$P_0'(\boldsymbol{r}) = \int_{\mathbb{R}_+^N} \frac{2}{\pi^{\frac{N}{2}}}\mathrm{e}^{-\|\boldsymbol{y}\|_2^2}(\boldsymbol{r}\circ\boldsymbol{y})^{\mathrm{T}}\mathrm{E}[\boldsymbol{x}]\mathrm{d}\boldsymbol{y} = \frac{1}{2^N}\frac{2}{\sqrt{\pi}}\boldsymbol{r}^{\mathrm{T}}\mathrm{E}[\boldsymbol{x}], \quad (89)$$

while the second order derivative reads as

$$\begin{aligned} &P_0''(\boldsymbol{r}) \\ &= \mathrm{E}_{\boldsymbol{x}}\int_{\mathbb{R}_+^N} \frac{2}{\pi^{N/2}}\mathrm{e}^{-\|\boldsymbol{y}\|_2^2}\left(2((\boldsymbol{r}\circ\boldsymbol{y})^{\mathrm{H}}\boldsymbol{x})^2 - \|\boldsymbol{x}\|_2^2\right)\mathrm{d}\boldsymbol{y} \\ &= \mathrm{E}_{\boldsymbol{x}}\int_{\mathbb{R}_+^N} \frac{2}{\pi^{N/2}}\mathrm{e}^{-\|\boldsymbol{y}\|_2^2}\left(\boldsymbol{x}^{\mathrm{T}}\left(2(\boldsymbol{r}\circ\boldsymbol{y})(\boldsymbol{r}\circ\boldsymbol{y})^{\mathrm{T}} - \mathbf{1}\right)\boldsymbol{x}\right)\mathrm{d}\boldsymbol{y} \\ &= \frac{1}{2^N}\frac{4}{\pi}\mathrm{E}\left[\boldsymbol{x}^{\mathrm{T}}\mathrm{nondiag}\left(\boldsymbol{r}\boldsymbol{r}^{\mathrm{T}}\right)\boldsymbol{x}\right] \\ &= \frac{1}{2^N}\frac{4}{\pi}\boldsymbol{r}^{\mathrm{T}}\mathrm{nondiag}\left(\mathrm{E}[\boldsymbol{x}\boldsymbol{x}^{\mathrm{T}}]\right)\boldsymbol{r}, \end{aligned} \quad (90)$$

where we used the following result

$$\int_{\mathbb{R}_+^N} \frac{\mathrm{e}^{-\|\boldsymbol{y}\|^2}}{\pi^{N/2}}(y_i\cdot r_i)(y_j\cdot r_j)\mathrm{d}\boldsymbol{y} = \begin{cases} \frac{1}{2\cdot 2^N} & \text{for } i=j \\ \frac{r_i r_j}{\pi\cdot 2^N} & \text{otherwise,} \end{cases} \quad (91)$$

and the relation $\mathrm{tr}(\mathrm{nondiag}(\boldsymbol{A})\boldsymbol{B}) = \mathrm{tr}(\boldsymbol{A}\mathrm{nondiag}(\boldsymbol{B}))$ for any two quadratic matrices $\boldsymbol{A}$ and $\boldsymbol{B}$.

In a similar way, we calculate $P_0^{(3)}(\boldsymbol{r})$

$$\begin{aligned} &P_0^{(3)}(\boldsymbol{r}) \quad (92) \\ &= \mathrm{E}_{\boldsymbol{x}}\int_{\mathbb{R}_+^N}\frac{6}{\pi^N}\mathrm{e}^{-\|\boldsymbol{y}\|_2^2}2((\boldsymbol{r}\circ\boldsymbol{y})^{\mathrm{T}}\boldsymbol{x}) \cdot\left(\frac{2}{3}((\boldsymbol{r}\circ\boldsymbol{y})^{\mathrm{T}}\boldsymbol{x})^2 - \|\boldsymbol{x}\|_2^2\right)\mathrm{d}\boldsymbol{y} \\ &= \mathrm{E}_{\boldsymbol{x}}\int_{\mathbb{R}_+^N}\left(\frac{8}{\pi^N}\mathrm{e}^{-\|\boldsymbol{y}\|_2^2}((\boldsymbol{r}\circ\boldsymbol{y})^{\mathrm{T}}\boldsymbol{x})^3 - \frac{12}{\pi^N}\mathrm{e}^{-\|\boldsymbol{r}\|_2^2}((\boldsymbol{r}\circ\boldsymbol{y})^{\mathrm{T}}\boldsymbol{x})\|\boldsymbol{x}\|_2^2\right)\mathrm{d}\boldsymbol{y} \\ &= \mathrm{E}_{\boldsymbol{x}}\int_{\mathbb{R}_+^N}\frac{8}{\pi^N}\mathrm{e}^{-\|\boldsymbol{y}\|_2^2}((\boldsymbol{r}\circ\boldsymbol{y})^{\mathrm{T}}\boldsymbol{x})^3\mathrm{d}\boldsymbol{y} - \frac{12}{2^N\sqrt{\pi}}\boldsymbol{r}^{\mathrm{T}}\mathrm{E}[\|\boldsymbol{x}\|_2^2\boldsymbol{x}] \\ &= \frac{1}{2^N}\frac{-4}{\sqrt{\pi}}\boldsymbol{r}^{\mathrm{T}}\mathrm{E}[\boldsymbol{x}\circ\boldsymbol{x}\circ\boldsymbol{x}] + \frac{12}{2^N\sqrt{\pi}}\boldsymbol{r}^{\mathrm{T}}\cdot\mathrm{E}[\|\boldsymbol{x}\|_2^2\cdot\boldsymbol{x}] \\ &\quad + \frac{48}{2^N}\frac{1}{\pi^{\frac{3}{2}}}\sum_{j\neq i, i\neq l, j\neq l}\mathrm{E}\left[r_i x_i r_j x_j r_l x_l\right] - \frac{12}{2^N\sqrt{\pi}}\boldsymbol{r}^{\mathrm{T}}\mathrm{E}[\|\boldsymbol{x}\|_2^2\boldsymbol{x}] \\ &= \frac{1}{2^N}\frac{-4}{\sqrt{\pi}}\boldsymbol{r}^{\mathrm{T}}\mathrm{E}[\boldsymbol{x}\circ\boldsymbol{x}\circ\boldsymbol{x}] + \frac{48}{2^N}\frac{1}{\pi^{\frac{3}{2}}}\sum_{j\neq i, i\neq l, j\neq l} r_i r_j r_l\mathrm{E}\left[x_i x_j x_l\right], \end{aligned} \quad (93)$$

[6]Since $\boldsymbol{x}$ is bounded in the coherent case due to the result in Appendix B (also due to practical limitations as well), we have that $p_\varepsilon^{(k)}(\boldsymbol{y})$ is bounded and exponentially decaying with respect to $\boldsymbol{y}$ and thus integrable on $\mathbb{R}_+^N$.

Authorized licensed use limited to: Access paid by The UC Irvine Libraries. Downloaded on May 08,2021 at 22:45:13 UTC from IEEE Xplore. Restrictions apply.

which follows from

$$\mathrm{E}_{\boldsymbol{x}} \int_{\mathbb{R}_+^N} \frac{8}{\pi^N} \mathrm{e}^{-\|\boldsymbol{y}\|_2^2} ((\boldsymbol{r} \circ \boldsymbol{y})^{\mathrm{T}} \boldsymbol{x})^3 \mathrm{d}\boldsymbol{y} =$$
$$= \frac{8}{\pi^N} \mathrm{E}_{\boldsymbol{x}} \int_{\mathbb{R}_+^N} \mathrm{e}^{-\|\boldsymbol{y}\|_2^2} (\sum_i r_i^3 y_i^3 x_i^3 + 3 \sum_{i,j\neq i} r_i^2 y_i^2 x_i^2 r_j y_j x_j$$
$$+ 6 \sum_{j\neq i\neq l} r_i y_i x_i r_j y_j x_j r_l y_l x_l) \mathrm{d}\boldsymbol{y}$$
$$= \frac{8}{2^N} \mathrm{E}_{\boldsymbol{x}} \left[\sum_i r_i \frac{1}{\sqrt{\pi}} x_i^3 + 3 \sum_{i,j\neq i} \frac{1}{2} x_i^2 r_j \frac{1}{\sqrt{\pi}} x_j \right.$$
$$\left. +6 \sum_{j\neq i\neq l} r_i \frac{1}{\sqrt{\pi}} x_i r_j \frac{1}{\sqrt{\pi}} x_j r_l \frac{1}{\sqrt{\pi}} x_l \right]$$
$$= \frac{8}{2^N} \mathrm{E}_{\boldsymbol{x}} \left[-\frac{1}{2} \sum_i r_i \frac{1}{\sqrt{\pi}} x_i^3 + \frac{3}{2} \sum_{i,j} x_i^2 r_j \frac{1}{\sqrt{\pi}} x_j \right.$$
$$\left. +6 \sum_{j\neq i\neq l} r_i \frac{1}{\sqrt{\pi}} x_i r_j \frac{1}{\sqrt{\pi}} x_j r_l \frac{1}{\sqrt{\pi}} x_l \right]$$
$$= -\frac{4}{2^N} \mathrm{E}_{\boldsymbol{x}} (\boldsymbol{r}^{\mathrm{T}} \mathrm{E}[\boldsymbol{x} \circ \boldsymbol{x} \circ \boldsymbol{x}]) + \frac{12}{2^N \sqrt{\pi}} \boldsymbol{r}^{\mathrm{T}} \cdot \mathrm{E}[\|\boldsymbol{x}\|_2^2 \cdot \boldsymbol{x}]$$
$$+ \frac{48}{2^N} \frac{1}{\pi^{\frac{3}{2}}} \sum_{j\neq i, i\neq l, j\neq l} \mathrm{E}\left[r_i x_i r_j x_j r_l x_l \right]. \quad (94)$$

Now, after the derivation of the derivatives $P_0'(\boldsymbol{r})$, $P_0''(\boldsymbol{r})$ and $P_0^{(3)}(\boldsymbol{r})$, we have to perform a summation with respect to $\boldsymbol{r} \in \{-1,+1\}^N$ of the terms given in (84). For this, we make use of the following properties:

$$\frac{1}{2^N} \sum_{\boldsymbol{r}\in\{-1,+1\}^N} \boldsymbol{r}^{\mathrm{T}} \boldsymbol{A} \boldsymbol{r} = \mathrm{tr}(\boldsymbol{A}), \quad (95)$$

and

$$\frac{1}{2^N} \sum_{\boldsymbol{r}\in\{-1,+1\}^N} \boldsymbol{r}^{\mathrm{T}} \boldsymbol{A} \boldsymbol{r} \cdot \boldsymbol{r}^{\mathrm{T}} \boldsymbol{B} \boldsymbol{r}$$
$$= \mathrm{tr}(\boldsymbol{A} \cdot \mathrm{nondiag}(\boldsymbol{B} + \boldsymbol{B}^{\mathrm{T}})) + \mathrm{tr}(\boldsymbol{A}) \mathrm{tr}(\boldsymbol{B}), \quad (96)$$

which can be verified by expanding the left-hand side and identifying the non-zero terms. We start by the second order expression of (84)

$$\sum_{\boldsymbol{r}\in\{-1,+1\}^N} \frac{P_0'(\boldsymbol{r})^2}{2P_0(\boldsymbol{r})} = \sum_{\boldsymbol{r}\in\{-1,+1\}^N} \frac{2}{2^N \cdot \pi} (\boldsymbol{r}^{\mathrm{T}} \mathrm{E}[\boldsymbol{x}]^{\mathrm{T}})^2$$
$$= \sum_{\boldsymbol{r}\in\{-1,+1\}^N} \frac{2}{2^N \cdot \pi} \boldsymbol{r}^{\mathrm{T}} \underbrace{\mathrm{E}[\boldsymbol{x}] \mathrm{E}[\boldsymbol{x}]^{\mathrm{T}}}_{\boldsymbol{A}} \boldsymbol{r}$$
$$= \frac{2}{\pi} \|\boldsymbol{x}\|_2^2. \quad (97)$$

Then, we consider the different terms of the fourth-order derivatives, starting with

$$\sum_{\boldsymbol{r}\in\{-1,+1\}^N} \frac{P_0'(\boldsymbol{r})^4}{12 P_0(\boldsymbol{r})^3}$$
$$= \sum_{\boldsymbol{r}\in\{-1,+1\}^N} \frac{4}{2^N \cdot 3\pi^2} (\boldsymbol{r}^{\mathrm{T}} \mathrm{E}[\boldsymbol{x}]^{\mathrm{T}})^4$$
$$= \sum_{\boldsymbol{r}\in\{-1,+1\}^N} \frac{4}{2^N \cdot 3\pi^2} \boldsymbol{r}^{\mathrm{T}} \underbrace{\mathrm{E}[\boldsymbol{x}] \mathrm{E}[\boldsymbol{x}]^{\mathrm{T}}}_{\boldsymbol{A}} \boldsymbol{r} \boldsymbol{r}^{\mathrm{T}} \underbrace{\mathrm{E}[\boldsymbol{x}] \mathrm{E}[\boldsymbol{x}]^{\mathrm{T}}}_{\boldsymbol{B}} \boldsymbol{r}$$
$$= \frac{4}{\pi^2} \mathrm{tr}(\mathrm{nondiag}(\mathrm{E}[\boldsymbol{x}] \mathrm{E}[\boldsymbol{x}]^{\mathrm{T}})^2) + \frac{4}{3\pi^2} \|\mathrm{E}[\boldsymbol{x}]\|_4^4. \quad (98)$$

On the other hand, we have

$$\sum_{\boldsymbol{r}\in\{-1,+1\}^N} \frac{P_0''(\boldsymbol{r})^2}{8 P_0(\boldsymbol{r})}$$
$$= \sum_{\boldsymbol{r}\in\{-1,+1\}^N} \frac{2}{2^N \cdot \pi^2} \boldsymbol{r}^{\mathrm{T}} \mathrm{nondiag}\left(\mathrm{E}[\boldsymbol{x}\boldsymbol{x}^{\mathrm{T}}] \right)$$
$$\cdot \boldsymbol{r}\boldsymbol{r}^{\mathrm{T}} \mathrm{nondiag}\left(\mathrm{E}[\boldsymbol{x}\boldsymbol{x}^{\mathrm{T}}] \right) \boldsymbol{r}$$
$$= \frac{4}{\pi^2} \mathrm{tr}(\mathrm{nondiag}(\mathrm{E}[\boldsymbol{x}\boldsymbol{x}^{\mathrm{T}}])^2). \quad (99)$$

Next, we get

$$\sum_{\boldsymbol{r}\in\{-1,+1\}^N} \frac{P_0'(\boldsymbol{r})^2 P_0''(\boldsymbol{r})}{4 P_0(\boldsymbol{r})^2}$$
$$= \sum_{\boldsymbol{r}\in\{-1,+1\}^N} \frac{4}{2^N \cdot \pi^2} \boldsymbol{r}^{\mathrm{T}} \mathrm{nondiag}\left(\mathrm{E}[\boldsymbol{x}\boldsymbol{x}^{\mathrm{T}}] \right)$$
$$\cdot \boldsymbol{r}\boldsymbol{r}^{\mathrm{T}} \mathrm{nondiag}\left(\mathrm{E}[\boldsymbol{x}] \mathrm{E}[\boldsymbol{x}]^{\mathrm{T}} \right) \boldsymbol{r}$$
$$= \frac{8}{\pi^2} \mathrm{tr}(\mathrm{nondiag}(\mathrm{E}[\boldsymbol{x}] \mathrm{E}[\boldsymbol{x}]^{\mathrm{T}}) \mathrm{nondiag}(\mathrm{E}[\boldsymbol{x}\boldsymbol{x}^{\mathrm{T}}])). \quad (100)$$

Further, we obtain

$$\sum_{\boldsymbol{r}\in\{-1,+1\}^N} \frac{P_0'(\boldsymbol{r}) P_0^{(3)}(\boldsymbol{r})}{6 P_0(\boldsymbol{r})}$$
$$= \frac{1}{6 \cdot 2^N} \sum_{\boldsymbol{r}\in\{-1,+1\}^N} \left(\frac{2}{\sqrt{\pi}} \boldsymbol{r}^{\mathrm{T}} \mathrm{E}[\boldsymbol{x}] \right) \left(\frac{-4}{\sqrt{\pi}} (\boldsymbol{r}^{\mathrm{T}} \mathrm{E}[\boldsymbol{x} \circ \boldsymbol{x} \circ \boldsymbol{x}]) \right.$$
$$\left. + \frac{48}{2^N} \frac{1}{\pi^{\frac{3}{2}}} \sum_{j\neq i, i\neq l, j\neq l} r_i r_j r_l \mathrm{E}\left[x_i x_j x_l \right] \right)$$
$$= -\frac{4}{3\pi} \mathrm{E}[\boldsymbol{x}]^{\mathrm{T}} \cdot \mathrm{E}[\boldsymbol{x} \circ \boldsymbol{x} \circ \boldsymbol{x}]$$
$$+ \frac{16}{\pi^2} \sum_{\boldsymbol{r}\in\{\pm 1\}^N} \sum_{j\neq i, i\neq l, j\neq l, k} r_i r_j r_l r_k \mathrm{E}[x_k] \mathrm{E}\left[x_i x_j x_l \right]$$
$$= -\frac{4}{3\pi} \mathrm{E}[\boldsymbol{x}]^{\mathrm{T}} \cdot \mathrm{E}[\boldsymbol{x} \circ \boldsymbol{x} \circ \boldsymbol{x}] + 0. \quad (101)$$

We plug the results from (97)–(101) into the expression for the entropy in (84), to get finally

$$H(\mathrm{sign}(\varepsilon \boldsymbol{x} + \boldsymbol{\eta})) = 2N \ln 2 - \frac{2}{\pi} \varepsilon^2 \|\mathrm{E}[\boldsymbol{x}]\|_2^2$$
$$- \varepsilon^4 \left(\frac{4}{\pi^2} \mathrm{tr}\left((\mathrm{nondiag}(\boldsymbol{C}_{\boldsymbol{x}}))^2 \right) + \frac{4}{3\pi^2} \|\mathrm{E}[g(\boldsymbol{x})]\|_4^4 \right.$$
$$\left. - \frac{4}{3\pi} \|\mathrm{E}[\boldsymbol{x}] \circ \mathrm{E}[\boldsymbol{x} \circ \boldsymbol{x} \circ \boldsymbol{x}]\|_1^1 \right) + \Delta H(\mathrm{sign}(\varepsilon \boldsymbol{x} + \boldsymbol{\eta})). \quad (102)$$

Now, for the complex-valued case, we easily obtain a similar result, since any N-dimensional vector can be represented as a real-valued $2N$-dimensional vector, where we split the vector into the real part and the imaginary part and write them as:

$$\boldsymbol{x}^r = \begin{bmatrix} \mathrm{Re}\{x\} \\ \mathrm{Im}\{x\} \end{bmatrix}. \quad (103)$$

Authorized licensed use limited to: Access paid by The UC Irvine Libraries. Downloaded on May 08,2021 at 22:45:13 UTC from IEEE Xplore. Restrictions apply.

This implies that the vector norms can be defined as

$$\|x\|_4^4 = \sum_k \mathrm{Re}\{x_k\}^4 + \mathrm{Im}\{x_k\}^4. \tag{104}$$

On the other hand, the covariance matrix can be written as

$$C_{x} = \mathrm{E}[xx^{\mathrm{H}}] - \mathrm{E}[x]\mathrm{E}[x^{\mathrm{H}}]. \tag{105}$$

Under the assumption that x is circularly distributed, i.e., $\mathrm{E}[xx^{\mathrm{T}}] = \mathrm{E}[x][x^{\mathrm{T}}]$, then we have

$$C_{x^r} = \mathrm{E}[x^r x^{r,\mathrm{T}}] = \frac{1}{2}\begin{bmatrix} \mathrm{Re}\{C_x\} & \mathrm{Im}\{C_x\} \\ -\mathrm{Im}\{C_x\} & \mathrm{Re}\{C_x\} \end{bmatrix}, \tag{106}$$

where we note that the matrix $\mathrm{Im}\{C_x\}$ is a skew-symmetric matrix, i.e., $\mathrm{Im}\{C_x^{\mathrm{T}}\} = -\mathrm{Im}\{C_x\}$ and has diagonal elements equal to zero, thus we have

$$\begin{aligned}
&(\mathrm{nondiag}(C_{x^r}))^2 \\
&= \frac{1}{2}(\mathrm{nondiag}(\mathrm{Re}\{C_x\}))^2 - \frac{1}{2}(\mathrm{Im}\{C_x\})^2 \\
&= \frac{1}{2}(\mathrm{nondiag}(\mathrm{Re}\{C_x\}))^2 - \frac{1}{2}(\mathrm{nondiag}(\mathrm{Im}\{C_x\}))^2 \\
&= \frac{1}{2}(\mathrm{nondiag}(C_x))^2.
\end{aligned} \tag{107}$$

Therefore, we can conclude that the formula remains the same except that we replace $(\mathrm{nondiag}(\mathrm{E}[xx^{\mathrm{H}}]))^2$ by $\frac{1}{2}(\mathrm{nondiag}(\mathrm{E}[xx^{\mathrm{H}}]))^2$, and the norms retain their same definition.

Now, we turn to the question of the conditions such that the second order approximation is valid. The condition $\mathrm{E}_x[\|x\|_4^{4+\alpha}] < \gamma$ for some finite constants $\alpha, \gamma > 0$ stated by the theorem ensures, similarly to the unquantized case [51], that the remainder term of the expansion given by

$$\Delta H(\mathrm{sign}(\varepsilon x + \eta)) = \mathrm{E}_x[o(\|x\|_4^4 \varepsilon^4)] \tag{108}$$

satisfies

$$\lim_{\varepsilon^4 \to 0} \frac{\Delta H(\mathrm{sign}(\varepsilon x + \eta))}{\varepsilon^4} = 0,$$

since the fifth oder derivative with respect ε exists and (similarly to the unquantized case in [51, Theorem 5])

$$\begin{aligned}
&|\Delta H(\mathrm{sign}(\varepsilon x + \eta))| \\
&= \mathrm{E}_x[o(\|x\|_4^4 \varepsilon^4)] \\
&\leq \mathrm{E}_x[(\|x\|_4^4 \varepsilon^4)^{1+\frac{\alpha'}{4}}], \text{ for some } \alpha' \in]0, \alpha] \\
&\leq \mathrm{E}_x[\|x\|_4^{4+\alpha'}]\varepsilon^{4+\alpha'} \\
&\leq \mathrm{E}_x[\|x\|_4^{4+\alpha}]^{\frac{4+\alpha'}{4+\alpha}} \varepsilon^{4+\alpha'} \text{(Hölder's inequality)} \\
&\leq \gamma^{\frac{4+\alpha'}{4+\alpha}} \varepsilon^{4+\alpha'} \\
&= o(\varepsilon^4).
\end{aligned} \tag{109}$$

This yields the result stated by the theorem and completes the proof.

Appendix B
Boundedness of the Support of the Capacity-Achieving Distribution

For simplicity, we consider a real-valued system since generalizing the result to the complex-valued case follows directly from its real-valued representation. Due to the concavity of the mutual information, the sufficient and necessary *Karush-Kuhn-Tucker* condition for an input distribution $p^*(x)$ to achieve the capacity C under the average power constraint $\mathrm{E}[\|x\|_2^2] \leq P_{\mathrm{Tr}}$ is that there exists $\lambda \geq 0$ such that [63]

$$\lambda(\|x\|_2^2 - P_{\mathrm{Tr}}) + C - \sum_r P(r|x)\log_2 \frac{P(r|x)}{P(r)} \geq 0, \ \forall x, \tag{110}$$

with equality if $p^*(x) > 0$. The idea for proving that the optimal distribution has bounded support is to show that the KL-distance

$$D(P(r|x)\|P(r)) = \sum_r P(r|x)\log_2 \frac{P(r|x)}{P(r)} \tag{111}$$

is always finite and therefore the equality in (110) can only hold with equality for finite $\|x\|_2^2$, in a similar manner to [47]. We bound this term as follows

$$\begin{aligned}
&\left|\sum_r P(r|x)\log_2 \frac{P(r|x)}{P(r)}\right| \\
&\leq \left|\sum_r P(r|x)\log_2 P(r|x)\right| + \left|\sum_r P(r|x)\log_2 P(r)\right| \\
&\leq N + \left|\sum_r P(r|x)\log_2 P(r)\right| \\
&\leq N + \left|\sum_r \log_2 P(r)\right| \\
&= N + \sum_r |\log_2 P(r)| \\
&= N - \sum_r \log_2 P(r) \\
&= N - \sum_{r \in \{\pm 1\}^N} \log_2 \mathrm{E}_x\left[\Pi_{i=1}^N \Phi\left(r_i \tilde{h}_i^{\mathrm{T}} x / \sqrt{\sigma_\eta^2/2}\right)\right] \\
&\leq N - 2^N \log_2 \mathrm{E}_x\left[\Pi_{i=1}^N \Phi\left(-|\tilde{h}_i^{\mathrm{T}} x| / \sqrt{\sigma_\eta^2/2}\right)\right] \\
&\leq N - 2^N \log_2 \mathrm{E}_x\left[\Pi_{i=1}^N \Phi\left(-\|\tilde{h}_i\|_2 \|x\|_2 / \sqrt{\sigma_\eta^2/2}\right)\right] \\
&\leq N - 2^N \log_2 \mathrm{E}_x\left[\Phi\left(-(\max_i \|\tilde{h}_i\|_2)\|x\|_2 / \sqrt{\sigma_\eta^2/2}\right)^N\right],
\end{aligned} \tag{112}$$

where $\tilde{h}_i^{\mathrm{T}}$ is the i-th row of the channel matrix $\tilde{H}$. Using the fact that $\Phi(-\sqrt{\rho})^N$, $\rho \geq 0$ is a convex function, since

$$\begin{aligned}
\frac{\mathrm{d}^2 \Phi(-\sqrt{\rho})^N}{\mathrm{d}\rho^2} &= N(N-1)\left(\frac{\mathrm{d}\Phi(-\sqrt{\rho})}{\mathrm{d}\rho}\right)^2 \Phi(-\sqrt{\rho})^{N-2} \\
&\quad + N\Phi(-\sqrt{\rho})^{N-1} \frac{\mathrm{e}^{-\frac{\rho}{2}}(1+\rho)}{4\sqrt{2\pi}\rho^{\frac{3}{2}}} \geq 0,
\end{aligned} \tag{113}$$

Authorized licensed use limited to: Access paid by The UC Irvine Libraries. Downloaded on May 08,2021 at 22:45:13 UTC from IEEE Xplore. Restrictions apply.

we obtain by Jensen's inequality

$$\begin{aligned}&\left|\sum_{\boldsymbol{r}} P(\boldsymbol{r}|\boldsymbol{x})\log_2\frac{P(\boldsymbol{r}|\boldsymbol{x})}{P(\boldsymbol{r})}\right|\\ &\leq N-2^N\log_2 \mathrm{E}_{\boldsymbol{x}}\left[\Phi\left(-(\max_i\|\tilde{\boldsymbol{h}}_i\|_2)\|\boldsymbol{x}\|_2/\sqrt{\sigma_\eta^2/2}\right)^N\right]\\ &\leq N-2^N\log_2\Phi\left(-(\max_i\|\tilde{\boldsymbol{h}}_i\|_2)\sqrt{\mathrm{E}_{\boldsymbol{x}}[\|\boldsymbol{x}\|_2^2]}/\sqrt{\sigma_\eta^2/2}\right)^N\\ &=N-2^N\cdot N\log_2\Phi\left(-(\max_i\|\tilde{\boldsymbol{h}}_i\|_2)\sqrt{2P_{\mathrm{Tr}}}/\sigma_\eta\right)\\ &<\infty, \end{aligned} \tag{114}$$

which is bounded if the channel is bounded. This ensures that (110) holds, for $\lambda \neq 0$, with equality only for finite $\|\boldsymbol{x}\|_2^2$ and thus the support of the capacity-achieving distribution is bounded if the power constraint is active.

Now we consider the case $\lambda = 0$, i.e., where the power constraint is inactive, and we assume without loss of generality that $\boldsymbol{x} \notin \mathrm{Null}(\tilde{\boldsymbol{H}})$ (null space does not contribute to the information transfer). From (112), we have that, for the capacity-achieving distribution, the output distribution satisfies $0 < P(\boldsymbol{r}) < 1$, since $\sum_{\boldsymbol{r}} |\log_2 P(\boldsymbol{r})|$ is finite (see (112) and (114)). Further, we write any possible input vector as $\boldsymbol{x} = \xi\hat{\boldsymbol{x}}$ for some $\xi > 0$ and $\hat{\boldsymbol{x}}$ having finite ℓ_2 norm. With larger input amplitude ξ, the support of the conditional output distribution $P(\boldsymbol{r}|\xi\hat{\boldsymbol{x}}) = \Pi_{i=1}^N \Phi\left(r_i\tilde{\boldsymbol{h}}_i^{\mathrm{T}}\sqrt{2}\xi\hat{\boldsymbol{x}}/\sigma_\eta\right) < 0.5^{N-\|\tilde{\boldsymbol{H}}\hat{\boldsymbol{x}}\|_0}$ reduces asymptotically to the set of outputs $\mathcal{S}_0 = \{\boldsymbol{r} \mid r_i\tilde{\boldsymbol{h}}_i^{\mathrm{T}}\hat{\boldsymbol{x}} \geq 0,\ \forall i\}$, i.e., since $\lim_{\tau\to\infty}\Phi(\tau) = 1$, $\lim_{\tau\to\infty}\Phi(-\tau) = 0$, and $\Phi(0) = 1/2$, we have

$$\begin{aligned}\lim_{\xi\to\infty} P(\boldsymbol{r}|\xi\hat{\boldsymbol{x}}) &= \lim_{\xi\to\infty}\Pi_{i=1}^N\Phi\left(r_i\tilde{\boldsymbol{h}}_i^{\mathrm{T}}\sqrt{2}\xi\hat{\boldsymbol{x}}/\sigma_\eta\right)\\ &=\begin{cases}0.5^{N-\|\tilde{\boldsymbol{H}}\hat{\boldsymbol{x}}\|_0}, & \text{for } \boldsymbol{r}\in\mathcal{S}_0\\ 0, & \text{otherwise.}\end{cases}\end{aligned}$$

Therefore, for $\xi \geq \xi_M$, with some sufficiently large ξ_M, we have, by uniform convergence, $0 < P(\boldsymbol{r}|\xi\hat{\boldsymbol{x}}) < 0.5^{N-\|\tilde{\boldsymbol{H}}\hat{\boldsymbol{x}}\|_0}P(\boldsymbol{r})$, $\forall \boldsymbol{r} \notin \mathcal{S}_0$. Consequently, we have

$$\begin{aligned}&D(P(\boldsymbol{r}|\xi\hat{\boldsymbol{x}})\|P(\boldsymbol{r}))\\ &=\sum_{\boldsymbol{r}} P(\boldsymbol{r}|\xi\hat{\boldsymbol{x}})\log_2\frac{P(\boldsymbol{r}|\xi\hat{\boldsymbol{x}})}{P(\boldsymbol{r})}\\ &=\sum_{\boldsymbol{r}} P(\boldsymbol{r}|\xi\hat{\boldsymbol{x}})\log_2\frac{0.5^{N-\|\tilde{\boldsymbol{H}}\hat{\boldsymbol{x}}\|_0}P(\boldsymbol{r}|\xi\hat{\boldsymbol{x}})}{0.5^{N-\|\tilde{\boldsymbol{H}}\hat{\boldsymbol{x}}\|_0}P(\boldsymbol{r})}\\ &=-(N-\|\tilde{\boldsymbol{H}}\hat{\boldsymbol{x}}\|_0)+\sum_{\boldsymbol{r}} P(\boldsymbol{r}|\xi\hat{\boldsymbol{x}})\log_2\frac{P(\boldsymbol{r}|\xi\hat{\boldsymbol{x}})}{0.5^{N-\|\tilde{\boldsymbol{H}}\hat{\boldsymbol{x}}\|_0}P(\boldsymbol{r})}\\ &=-(N-\|\tilde{\boldsymbol{H}}\hat{\boldsymbol{x}}\|_0)+\underbrace{\sum_{\boldsymbol{r}\in\mathcal{S}_0} P(\boldsymbol{r}|\xi\hat{\boldsymbol{x}})\log_2\frac{P(\boldsymbol{r}|\xi\hat{\boldsymbol{x}})}{0.5^{N-\|\tilde{\boldsymbol{H}}\hat{\boldsymbol{x}}\|_0}P(\boldsymbol{r})}}_{\text{Term 1}}\\ &\quad+\underbrace{\sum_{\boldsymbol{r}\notin\mathcal{S}_0} P(\boldsymbol{r}|\xi\hat{\boldsymbol{x}})\log_2\frac{P(\boldsymbol{r}|\xi\hat{\boldsymbol{x}})}{0.5^{N-\|\tilde{\boldsymbol{H}}\hat{\boldsymbol{x}}\|_0}P(\boldsymbol{r})}}_{\text{Term 2}}.\end{aligned} \tag{115}$$

Term 2 in (115) becomes strictly negative for $\xi > \xi_M$ since $\forall \boldsymbol{r} \in \mathcal{S}_0$, $P(\boldsymbol{r}|\xi\hat{\boldsymbol{x}}) < 0.5^{N-\|\tilde{\boldsymbol{H}}\hat{\boldsymbol{x}}\|_0}P(\boldsymbol{r})$. As a result, for $\xi > \xi_M$, we obtain

$$\begin{aligned}&D(P(\boldsymbol{r}|\xi\hat{\boldsymbol{x}})\|P(\boldsymbol{r}))|_{\xi>\xi_M}\\ &<-(N-\|\tilde{\boldsymbol{H}}\hat{\boldsymbol{x}}\|_0)+\sum_{\boldsymbol{r}\in\mathcal{S}_0} P(\boldsymbol{r}|\xi\hat{\boldsymbol{x}})\log_2\frac{P(\boldsymbol{r}|\xi\hat{\boldsymbol{x}})}{0.5^{N-\|\tilde{\boldsymbol{H}}\hat{\boldsymbol{x}}\|_0}P(\boldsymbol{r})}\\ &<-(N-\|\tilde{\boldsymbol{H}}\hat{\boldsymbol{x}}\|_0)+\sum_{\boldsymbol{r}\in\mathcal{S}_0} 0.5^{N-\|\tilde{\boldsymbol{H}}\hat{\boldsymbol{x}}\|_0}\log_2\frac{1}{P(\boldsymbol{r})}\\ &\qquad\qquad(\text{since } P(\boldsymbol{r}|\xi\hat{\boldsymbol{x}}) < 0.5^{N-\|\tilde{\boldsymbol{H}}\hat{\boldsymbol{x}}\|_0})\\ &=\sum_{\boldsymbol{r}\in\mathcal{S}_0} 0.5^{N-\|\tilde{\boldsymbol{H}}\hat{\boldsymbol{x}}\|_0}\log_2\frac{0.5^{N-\|\tilde{\boldsymbol{H}}\hat{\boldsymbol{x}}\|_0}}{P(\boldsymbol{r})}\\ &=\lim_{\xi\to\infty} D(P(\boldsymbol{r}|\xi\hat{\boldsymbol{x}})\|P(\boldsymbol{r}))\\ &\leq C,\end{aligned} \tag{116}$$

where the last step follows due to the KKT condition (110) for $\lambda = 0$. Since $D(P(\boldsymbol{r}|\xi\hat{\boldsymbol{x}})\|P(\boldsymbol{r})) < C$ for $\xi > \xi_M$, $\boldsymbol{x} = \xi\hat{\boldsymbol{x}}$ cannot be part of the support of the capacity-achieving distribution for $\infty > \xi \geq \xi_M$ and $\hat{\boldsymbol{x}}$ having finite ℓ_2 norm. This completes the proof for both cases $\lambda = 0$ and $\lambda > 0$.

Acknowledgment

The authors would like to thank the anonymous reviewers for their suggestions and contributions that substantially improved the quality of the article. Parts of this work were published in [1]–[3], where some proofs were missing, and in particular, the main theorem in Section III was not stated and the application to massive MIMO was not investigated.

References

[1] A. Mezghani and J. A. Nossek, "On ultra-wideband MIMO systems with 1-bit quantized outputs: Performance analysis and input optimization," in *Proc. IEEE Int. Symp. Inf. Theory*, Jun. 2007, pp. 1286–1289.
[2] A. Mezghani and J. A. Nossek, "Analysis of Rayleigh-fading channels with 1-bit quantized output," in *Proc. IEEE Int. Symp. Inf. Theory*, Jul. 2008, pp. 260–264.
[3] A. Mezghani and J. A. Nossek, "Analysis of 1-bit output noncoherent fading channels in the low SNR regime," in *Proc. IEEE Int. Symp. Inf. Theory*, Jun. 2009, pp. 1080–1084.
[4] T. L. Marzetta, "Noncooperative cellular wireless with unlimited numbers of base station antennas," *IEEE Trans. Wireless Commun.*, vol. 9, no. 11, pp. 3590–3600, Nov. 2010.
[5] L. Lu, G. Y. Li, A. L. Swindlehurst, A. Ashikhmin, and R. Zhang, "An overview of massive MIMO: Benefits and challenges," *IEEE J. Sel. Topics Signal Process.*, vol. 8, no. 5, pp. 742–758, Oct. 2014.
[6] U. Madhow, "MultiGigabit millimeter wave communication: System concepts and challenges," in *Proc. Inf. Theory Appl. Workshop*, Jan. 2008, pp. 193–196.
[7] F. Boccardi, R. W. Heath, Jr., A. Lozano, T. L. Marzetta, and P. Popovski, "Five disruptive technology directions for 5G," *IEEE Commun. Mag.*, vol. 52, no. 2, pp. 74–80, Feb. 2014.
[8] A. L. Swindlehurst, E. Ayanoglu, P. Heydari, and F. Capolino, "Millimeter-wave massive MIMO: The next wireless revolution?" *IEEE Commun. Mag.*, vol. 52, no. 9, pp. 56–62, Sep. 2014.
[9] W. Roh *et al.*, "Millimeter-wave beamforming as an enabling technology for 5G cellular communications: Theoretical feasibility and prototype results," *IEEE Commun. Mag.*, vol. 52, no. 2, pp. 106–113, Feb. 2014.
[10] S. Rangan, T. S. Rappaport, and E. Erkip, "Millimeter-wave cellular wireless networks: Potentials and challenges," *Proc. IEEE*, vol. 102, no. 3, pp. 366–385, Mar. 2014.
[11] M. T. Ivrlač and J. A. Nossek, "Challenges in coding for quantized MIMO systems," in *Proc. IEEE Int. Symp. Inf. Theory*, Jul. 2006, pp. 2114–2118.

Authorized licensed use limited to: Access paid by The UC Irvine Libraries. Downloaded on May 08,2021 at 22:45:13 UTC from IEEE Xplore. Restrictions apply.

[12] B. M. Murray and I. B. Collings, "AGC and quantization effects in a zero-forcing MIMO wireless system," in *Proc. IEEE 63rd Veh. Technol. Conf.*, vol. 4, May 2006, pp. 1802–1806.

[13] B. M. Murray, "Maximizing the cutoff rate in a quantized MIMO wireless system with AGC," in *Proc. Int. Conf. Wireless Broadband Ultra Wideband Commun.*, Sydney, NSW, Australia, Mar. 2006, pp. 6–10.

[14] A. J. Nossek and M. T. Ivrlač, "Capacity and Coding for Quantized MIMO Systems," in *Proc. Int. Conf. Wireless Commun. Mobile Comput. (IWCMC)*, New York, NY, USA, 2006, pp. 1387–1392, doi: 10.1145/1143549.1143827.

[15] A. Mezghani, M. S. Khoufi, and J. A. Nossek, "A modified MMSE receiver for quantized MIMO systems," in *Proc. ITG Workshop Smart Antennas (WSA)*, Feb. 2007, pp 1–5.

[16] A. Mezghani, M.-S. Khoufi, and J. A. Nossek, "Spatial MIMO decision feedback equalizer operating on quantized data," in *Proc. IEEE Int. Conf. Acoust., Speech Signal Process.*, Mar. 2008, pp. 2893–2896.

[17] A. Mezghani, F. Antreich, and J. A. Nossek, "Multiple parameter estimation with quantized channel output," in *Proc. Int. ITG Workshop Smart Antennas (WSA)*, Feb. 2010, pp. 143–150.

[18] T. Koch and A. Lapidoth, "At low SNR, asymmetric quantizers are better," *IEEE Trans. Inf. Theory*, vol. 59, no. 9, pp. 5421–5445, Sep. 2013.

[19] J. Singh, O. Dabeer, and U. Madhow, "On the limits of communication with low-precision analog-to-digital conversion at the receiver," *IEEE Trans. Commun.*, vol. 57, no. 12, pp. 3629–3639, Dec. 2009.

[20] J. Singh, O. Dabeer, and U. Madhow, "Capacity of the discrete-time AWGN channel under output quantization," in *Proc. IEEE Int. Symp. Inf. Theory*, Jul. 2008, pp. 1218–1222.

[21] G. Zeitler, A. C. Singer, and G. Kramer, "Low-precision A/D conversion for maximum information rate in channels with memory," *IEEE Trans. Commun.*, vol. 60, no. 9, pp. 2511–2521, Sep. 2012.

[22] K. Nakamura and T. Tanaka, "Performance analysis of signal detection using quantized received signals of linear vector channel," in *Proc. Int. Symp. Inf. Theory Appl.*, Dec. 2008, pp. 1–5.

[23] A. Mezghani and J. A. Nossek, "Belief propagation based MIMO detection operating on quantized channel output," in *Proc. IEEE Int. Symp. Inf. Theory*, Jun. 2010, pp. 2113–2117.

[24] A. Mezghani, M. S. Khoufi, and J. A. Nossek, "Maximum likelihood detection for quantized MIMO systems," in *Proc. Int. ITG Workshop Smart Antennas*, Feb. 2008, pp. 278–284.

[25] A. Mezghani and J. A. Nossek, "Capacity lower bound of MIMO channels with output quantization and correlated noise," in *Proc. IEEE Int. Symp. Inf. Theory*, Jul. 2012, pp. 1–5. [Online]. Available: https://mediatum.ub.tum.de/doc/1171263/1171263.pdf

[26] S. Wang, Y. Li, and J. Wang, "Multiuser detection for uplink large-scale MIMO under one-bit quantization," in *Proc. IEEE Int. Conf. Commun. (ICC)*, Jun. 2014, pp. 4460–4465.

[27] S. Wang, Y. Li, and J. Wang, "Multiuser detection in massive spatial modulation MIMO with low-resolution ADCs," *IEEE Trans. Wireless Commun.*, vol. 14, no. 4, pp. 2156–2168, Apr. 2015.

[28] J. Mo and R. W. Heath, Jr., "Capacity analysis of one-bit quantized MIMO systems with transmitter channel state information," *IEEE Trans. Signal Process.*, vol. 63, no. 20, pp. 5498–5512, Oct. 2015.

[29] C. Studer and G. Durisi, "Quantized massive MU-MIMO-OFDM uplink," *IEEE Trans. Commun.*, vol. 64, no. 6, pp. 2387–2399, Jun. 2016.

[30] S. Jacobsson, G. Durisi, M. Coldrey, U. Gustavsson, and C. Studer, "Throughput analysis of massive MIMO uplink with low-resolution ADCs," *IEEE Trans. Wireless Commun.*, vol. 16, no. 6, pp. 4038–4051, Jun. 2017.

[31] J. Singh, S. Ponnuru, and U. Madhow, "Multi-Gigabit communication: The ADC bottleneck," in *Proc. IEEE Int. Conf. Ultra-Wideband*, Sep. 2009, pp. 22–27.

[32] A. Mezghani, M. Rouatbi, and J. A. Nossek, "An iterative receiver for quantized MIMO systems," in *Proc. 16th IEEE Medit. Electrotechn. Conf.*, Mar. 2012, pp. 1049–1052.

[33] J. Mo and R. W. Heath, Jr., "High SNR capacity of millimeter wave MIMO systems with one-bit quantization," in *Proc. Inf. Theory Appl. Workshop (ITA)*, Feb. 2014, pp. 1–5.

[34] C. Risi, D. Persson, and E. G. Larsson, "Massive MIMO with 1-bit ADC," 2014, *arXiv:1404.7736*. [Online]. Available: http://arxiv.org/abs/1404.7736

[35] J. Mo, P. Schniter, N. G. Prelcic, and R. W. Heath, Jr., "Channel estimation in millimeter wave MIMO systems with one-bit quantization," in *Proc. 48th Asilomar Conf. Signals, Syst. Comput.*, Nov. 2014, pp. 957–961.

[36] N. Liang and W. Zhang, "Mixed-ADC massive MIMO," *IEEE J. Sel. Areas Commun.*, vol. 34, no. 4, pp. 983–997, Apr. 2016.

[37] S. Jacobsson, G. Durisi, M. Coldrey, U. Gustavsson, and C. Studer, "One-bit massive MIMO: Channel estimation and high-order modulations," in *Proc. IEEE Int. Conf. Commun. Workshop (ICCW)*, Jun. 2015, pp. 1304–1309.

[38] J. Choi, J. Mo, and R. W. Heath, Jr., "Near maximum-likelihood detector and channel estimator for uplink multiuser massive MIMO systems with one-bit ADCs," *IEEE Trans. Commun.*, vol. 64, no. 5, pp. 2005–2018, May 2016.

[39] C.-K. Wen, S. Jin, K.-K. Wong, C.-J. Wang, and G. Wu, "Joint cHANNEL-AND-dATA estimation for large-MIMO systems with low-precision ADCs," in *Proc. IEEE Int. Symp. Inf. Theory (ISIT)*, Jun. 2015, pp. 1237–1241.

[40] C. Mollén, J. Choi, E. G. Larsson, and R. W. Heath, Jr., "Performance of linear receivers for wideband massive MIMO with one-bit ADCs," in *Proc. 20th Int. ITG Workshop Smart Antennas (WSA)*, Mar. 2016, pp. 1–7.

[41] C. Mollen, J. Choi, E. G. Larsson, and R. W. Heath, Jr., "One-bit ADCs in wideband massive MIMO systems with OFDM transmission," in *Proc. IEEE Int. Conf. Acoust., Speech Signal Process. (ICASSP)*, Mar. 2016, pp. 3386–3390.

[42] C. Mollén, J. Choi, E. G. Larsson, and R. W. Heath, Jr., "Uplink performance of wideband massive MIMO with one-bit ADCs," *IEEE Trans. Wireless Commun.*, vol. 16, no. 1, pp. 87–100, Jan. 2017.

[43] Y. Li, C. Tao, L. Liu, G. Seco-Granados, and A. L. Swindlehurst, "Channel estimation and uplink achievable rates in one-bit massive MIMO systems," in *Proc. IEEE Sensor Array Multichannel Signal Process. Workshop (SAM)*, Jul. 2016, pp. 1–5.

[44] Y. Li, C. Tao, L. Liu, A. Mezghani, and A. L. Swindlehurst, "How much training is needed in one-bit massive MIMO systems at low SNR?" in *Proc. IEEE Global Commun. Conf. (GLOBECOM)*, Dec. 2016, pp. 1–6.

[45] Y. Li, C. Tao, G. Seco-Granados, A. Mezghani, A. L. Swindlehurst, and L. Liu, "Channel estimation and performance analysis of one-bit massive MIMO systems," *IEEE Trans. Signal Process.*, vol. 65, no. 15, pp. 4075–4089, Aug. 2017.

[46] C. Stockle, J. Munir, A. Mezghani, and J. A. Nossek, "Channel estimation in massive MIMO systems using 1-bit quantization," in *Proc. IEEE 17th Int. Workshop Signal Process. Adv. Wireless Commun. (SPAWC)*, Jul. 2016, pp. 1–6.

[47] B. Rassouli, M. Varasteh, and D. Gündüz, "Gaussian multiple access channels with one-bit quantizer at the receiver," *Entropy*, vol. 20, no. 9, p. 686, 2018.

[48] I. D. O'Donnell and R. W. Brodersen, "An ultra-wideband transceiver architecture for low power, low rate, wireless systems," *IEEE Trans. Veh. Technol.*, vol. 54, no. 5, pp. 1623–1631, Sep. 2005.

[49] A. J. Viterbi and J. K. Omura, *Principles of Digital Communication and Coding*. New York, NY, USA: McGraw-Hill, 1979.

[50] S. Verdú, "Spectral efficiency in the wideband regime," *IEEE Trans. Inf. Theory*, vol. 48, no. 6, pp. 1319–1343, Jun. 2002.

[51] V. V. Prelov and S. Verdú, "Second-order asymptotics of mutual information," *IEEE Trans. Inf. Theory*, vol. 50, no. 8, pp. 1567–1580, Aug. 2004.

[52] C. Rao and B. Hassibi, "Analysis of multiple-antenna wireless links at low SNR," *IEEE Trans. Inf. Theory*, vol. 50, no. 9, pp. 2123–2130, Sep. 2004.

[53] X. Wu and R. Srikant, "MIMO channels in the low-SNR regime: Communication rate, error exponent, and signal peakiness," *IEEE Trans. Inf. Theory*, vol. 53, no. 4, pp. 1290–1309, Apr. 2007.

[54] V. Sethuraman, L. Wang, B. Hajek, and A. Lapidoth, "Low-SNR capacity of noncoherent fading channels," *IEEE Trans. Inf. Theory*, vol. 55, no. 4, pp. 1555–1574, Apr. 2009.

[55] G. Durisi, U. G. Schuster, H. Bolcskei, and S. Shamai (Shitz), "Noncoherent capacity of underspread fading channels," *IEEE Trans. Inf. Theory*, vol. 56, no. 1, pp. 367–395, Jan. 2010.

[56] L. Zheng and D. N. C. Tse, "Communication on the Grassmann manifold: A geometric approach to the noncoherent multiple-antenna channel," *IEEE Trans. Inf. Theory*, vol. 48, no. 2, pp. 359–383, Feb. 2002.

[57] T. Koch and A. Lapidoth, "Increased capacity per unit-cost by oversampling," in *Proc. IEEE 26th Conv. Electr. Electron. Eng. Isr.*, Nov. 2010, pp. 684–688.

[58] T. M. Cover and J. A. Thomas, *Elements of Information Theory*. New York, NY, USA: Wiley, 1991.

[59] R. H. Bacon, "Approximations to multivariate normal orthant probabilities," *Ann. Math. Statist.*, vol. 34, no. 1, pp. 191–198, Mar. 1963.

Authorized licensed use limited to: Access paid by The UC Irvine Libraries. Downloaded on May 08,2021 at 22:45:13 UTC from IEEE Xplore. Restrictions apply.

[60] T. L. Marzetta and B. M. Hochwald, "Capacity of a mobile multiple-antenna communication link in Rayleigh flat fading," *IEEE Trans. Inf. Theory*, vol. 45, no. 1, pp. 139–157, Jan. 1999.

[61] G. Winkler, "Extreme points of moment set," *Math. Oper. Res.*, vol. 13, no. 4, pp. 581–587, 1988.

[62] I. E. Telatar and D. N. C. Tse, "Capacity and mutual information of wideband multipath fading channels," *IEEE Trans. Inf. Theory*, vol. 46, no. 4, pp. 1384–1400, Jul. 2000.

[63] M. Fozunbal, S. W. McLaughlin, and R. W. Schafer, "Capacity analysis for continuous alphabet channels with side information, part II: MIMO channels," *IEEE Trans. Inf. Theory*, vol. 51, no. 9, pp. 3086–3101, Sep. 2005.

Amine Mezghani (Member, IEEE) received the Ph.D. degree in electrical engineering from the Technical University of Munich, Germany, in 2015. He is currently an Assistant Professor with the Department of Electrical and Computer Engineering, University of Manitoba, Canada. Prior to this, he was a Post-Doctoral Fellow with The University of Texas at Austin, USA, and a Post-Doctoral Scholar with the Department of Electrical Engineering and Computer Science, University of California at Irvine, USA. His current research interests include millimeter-wave communications, massive MIMO, hardware constrained radar and communication systems, antenna theory, and large-scale signal processing algorithms. He was a recipient of the joint Rohde & Schwarz and EE Department Outstanding Dissertation Award in 2016. He has published over 100 articles, particularly on the topic of signal processing and communications with low-resolution analog-to-digital and digital-to-analog converters.

Josef A. Nossek (Life Fellow, IEEE) received the Dipl.-Ing. and Dr.techn. degrees in electrical engineering from the Vienna University of Technology, Vienna, Austria, in 1974 and 1980, respectively. In 1974, he joined Siemens AG, Munich, Germany, where he was engaged in filter design for communication systems. From 1987 to 1989, he was the Head of the Radio Systems Design Department, where he was instrumental in introducing high-speed VLSI signal processing into digital microwave radio. From 1989 to 2016, he was a Full Professor of Circuit Theory and Signal Processing with the Technical University of Munich (TUM), Munich. Since 2016, he has been an Emeritus of Excellence of TUM and a Full Professor with the Federal University of Ceará, Fortaleza, Brazil. He was the President-Elect, President, and Past President of the IEEE Circuits and Systems Society in 2001, 2002, and 2003, respectively. He was the President of Verband der Elektrotechnik, Elektronik und Informationstechnik (VDE) from 2007 to 2008, and the President of the Convention of National Associations of Electrical Engineers of Europe (EUREL) in 2013. In 2009, he became a member of the National Academy of Engineering in Germany (acatech). He was a recipient of the ITG Best Paper Award in 1988, the Mannesmann Mobilfunk (currently Vodafone) Innovations Award in 1998, and the Award for Excellence in Teaching from the Bavarian Ministry for Science, Research and Art in 1998. From the IEEE Circuits and Systems Society, he was a recipient of the Golden Jubilee Medal for Outstanding Contributions to the Society in 1999 and the Education Award in 2008. He was also a recipient of the Order of Merit of the Federal Republic of Germany (Bundesverdienstkreuz am Bande) in 2008, the IEEE Guillemin-Cauer Best Paper Award in 2011, the Honorary Doctorate (Dr.h.c.) from the Peter Pazmany Catholic University, Hungary, in 2013, and the VDE Ring of Honor in 2014.

A. Lee Swindlehurst (Fellow, IEEE) received the B.S. and M.S. degrees in electrical engineering from Brigham Young University (BYU) in 1985 and 1986, respectively, and the Ph.D. degree in electrical engineering from Stanford University in 1991. He was with the Department of Electrical and Computer Engineering, BYU, from 1990 to 2007, where he served as the Department Chair from 2003 to 2006. From 1996 to 1997, he held a joint appointment as a Visiting Scholar at Uppsala University and the Royal Institute of Technology, Sweden. From 2006 to 2007, he was, on leave, working as the Vice President of Research for ArrayComm LLC, San Jose, CA, USA. Since 2007, he has been a Professor with the Electrical Engineering and Computer Science Department, University of California at Irvine, where he served as the Associate Dean for Research and Graduate Studies in the Samueli School of Engineering from 2013 to 2016. From 2014 to 2017, he was also a Hans Fischer Senior Fellow of the Institute for Advanced Studies, Technical University of Munich. His research interests include array signal processing for radar, wireless communications, and biomedical applications, and he has over 300 publications in these areas. In 2016, he was elected as a Foreign Member of the Royal Swedish Academy of Engineering Sciences (IVA). He received the 2000 IEEE W. R. G. Baker Prize Paper Award, the 2006 IEEE Communications Society Stephen O. Rice Prize in the Field of Communication Theory, the 2006 and 2010 IEEE Signal Processing Society's Best Paper Awards, and the 2017 IEEE Signal Processing Society Donald G. Fink Overview Paper Award. He was the inaugural Editor-in-Chief of the IEEE JOURNAL OF SELECTED TOPICS IN SIGNAL PROCESSING.

Authorized licensed use limited to: Access paid by The UC Irvine Libraries. Downloaded on May 08,2021 at 22:45:13 UTC from IEEE Xplore. Restrictions apply.